

# Cocycles of the space of long embeddings and BCR graphs with more than one loop

Leo Yoshioka\*

December 2022

## Abstract

The purpose of this paper is to construct non-trivial cocycles of the space  $\text{Emb}(\mathbb{R}^j, \mathbb{R}^n)$  of long embeddings. We construct the cocycles by integral over configuration spaces, associated with Bott-Cattaneo-Rossi graphs with more than one loop. As an application, we explicitly give a non-trivial family of trivial long embeddings for odd  $n, j$  with  $n-j \geq 2$  and  $j \geq 3$ . This family (cycle) is constructed from a chord diagram on directed lines. The non-triviality is shown by cocycle-cycle pairing, described by pairing between graphs and chord diagrams.

## Contents

<b>Introduction</b>	<b>2</b>
<b>1 Background</b>	<b>4</b>
1.1 $\text{Emb}_\partial(D^n, D^{n+2})$ and $\text{Diff}_\partial(D^{n+1} \times S^1)$	5
1.2 BCR graph complex and the de Rham complex of $\text{Emb}(\mathbb{R}^j, \mathbb{R}^n)$	5
<b>2 Definition</b>	<b>6</b>
2.1 The space of long embeddings	6
2.2 BCR graphs	7
2.3 BCR graph complex	9
2.4 Comparing with Arone-Turchin graph complex	11
2.5 Configuration space integral	12
<b>3 Main Result</b>	<b>14</b>

---

\*Graduate School of Mathematical Sciences, The University of Tokyo  
e-mail:yoshioka@ms.u-tokyo.ac.jp

<b>4</b>	<b>Construction of the cocycles</b>	<b>18</b>
4.1	H is a graph cocycle . . . . .	18
4.2	Vanishing of the contribution of hidden faces . . . . .	18
4.3	Construction of a correction term for anomalous faces . . . . .	21
<b>5</b>	<b>Construction of the cycles</b>	<b>24</b>
5.1	Planetary systems and chord diagrams on directed lines . . . . .	24
5.2	Construction of the cycles . . . . .	25
5.3	Perturbation of ribbon presentations . . . . .	30
5.4	Lifting the cycles to $\overline{\text{Emb}}(\mathbb{R}^j, \mathbb{R}^n)$ . . . . .	32
<b>6</b>	<b>Some lemmas for computing cocycle-cycle pairing</b>	<b>32</b>
<b>7</b>	<b>Proof of Main Result</b>	<b>38</b>
<b>8</b>	<b>Higher orders and higher loops</b>	<b>41</b>
8.1	The modified BCR graph complex . . . . .	41
8.2	Computation of some modified BCR graph cohomology . . . . .	43

# Introduction

A long embedding is an embedding of  $\mathbb{R}^j$  into  $\mathbb{R}^n$ , which is standard outside a disk in  $\mathbb{R}^j$ . A long  $n$ -knot is a long embedding  $\mathbb{R}^n \rightarrow \mathbb{R}^{n+2}$ . In this paper, we give some non-trivial cocycles of the space  $\text{Emb}(\mathbb{R}^j, \mathbb{R}^n)$  of long embeddings by integral associated with graphs. This kind of approach, which we call configuration space integral, has its quantum field theoretical origin in E. Witten's work [Wit] and its mathematical formulation has been developed by M. Kontsevich[Kon], D. Bar-Natan[Bar], R. Bott[Bot], C. Taubes[BT], G. Kuperberg, D. Thurston[KT], A. S. Cattaneo, C. A. Rossi[CR] and so on from the 1990s to 2000s. Recently, this approach again has been gathering attention, since T. Watanabe[Wat 5] in 2018, based on a series of his works [Wat 2][Wat 3][Wat 4], disproved 4-dimensional Smale conjecture.

Bott[Bot], Cattaneo and Rossi[CR] defined 1-loop graphs with two types of edges and vertices (BCR graphs). Using specific linear combinations of BCR graphs called graph cocycles, they defined configuration space integral invariants for long  $n$ -knots. Sakai and Watanabe [SW] generalized their construction and systematically gave non-trivial higher cocycles of  $\text{Emb}(\mathbb{R}^j, \mathbb{R}^n)$  for  $n - j \geq 3$  from BCR graph cocycles.

The graphs used in this paper are similar to theirs, but our graphs have more than one loop. Using such higher-loop graphs plays an essential role in getting cocycles of higher degree when the codimension  $n - j$  is exactly two. The framework of applying higher-loop BCR graphs was already considered by K. Sakai [Sak 2]. However, no non-trivial cocycle corresponding to higher-loop graphs has been given so far.

Our main focus is low dimensional cases:  $\text{Emb}(\mathbb{R}^n, \mathbb{R}^{n+2})$  for  $n = 2$  or  $3$ . The homotopy type of these spaces is mysterious, though recently great progress has been made by R. Budney and D. Gabai in [BG]. (See subsection 1.1.)

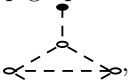
In this paper, we show the following. (See Section 3.)

**Theorem.** Let  $n, j$  be odd and satisfy  $n - j \geq 2, j \geq 3$ . Then the linear combination  $\overline{H_2}$  of 2-loop BCR graphs gives an explicit non-trivial  $3n - 2j - 7$  (co)cycle of  $\text{Emb}(\mathbb{R}^j, \mathbb{R}^n)$ , the space of long embeddings modulo immersions.

This theorem is shown by cocycle-cycle pairing. We systematically construct cycles of the space of long embeddings, which we call generalized ribbon cycles, from chord diagrams on directed lines. This diagrammatic construction makes it possible to compute cocycle-cycle pairing through pairing between graphs and diagrams. This diagrammatic computation is analog of the diagrammatic description of cohomology-homology pairing of configuration space that D.P. Sinha introduced in [Sin2].

As a corollary, we give a non-trivial  $S^2$  family of trivial long 3-knots. Budney and Gabai[BG] already showed  $\pi_{n-1}(\text{Emb}(\mathbb{R}^n, \mathbb{R}^{n+2})_u)$  has an infinite-rank subgroup, by different approaches from ours. However, since their families of long  $n$ -knots are constructed through  $\text{Diff}_\partial(D^{n+1} \times S^1)$  or  $\text{Emb}_\partial(D^1, D^{n+1} \times S^1)$ , it would be meaningful we get to know explicit geometric construction. At present, the author does not know the direct relation between the two families.

Moreover, our graph cocycles with more than one loop will further support the interesting similarity between BCR graph complex and the graph complex introduced by G. Arone and V. Turchin[AT1][AT2]. Their complex arises from homotopy theoretical approaches to the space of embeddings, the theory of embedding calculus, which Goodwillie, Klein and Weiss developed [GW][GKW][Wei], and the theory of operad. The significant point of their complex is that its graph homology has the whole dimensional information of rational homology of  $\text{Emb}(\mathbb{R}^j, \mathbb{R}^n)$  for  $n - j \geq 3$ <sup>1</sup>. They mentioned in [AT2] that some of their graphs are very similar to BCR graphs with no more than one loop. The point there was that Arone and Turchin's graph complex admits graphs with more than one loop. The 2-loop graph cocycle we give in this paper

has a similar graph to the 2-loop graph , which appears as a non-

trivial element in [AT2]. Since BCR graph cohomology can give information for any codimension more than one, we would be able to say that the stability of high codimension that is described by this graph also survives in the range  $n - j = 2$ .

Although we can construct some non-trivial higher-loop graph cocycles for even  $n, j$ , so far we have got no non-trivial cocycles of the space of long embeddings. This seems to be because these graph cocycles vanish after the relation

<sup>1</sup>In [FTW], Fresse, Turchin and Willwacher generalized [AT2] to  $n - j \geq 3$ . Note that their approach consists of (i) Goodwillie–Weiss embedding calculus tower (ii) its mapping space model. (ii) is applicable to any codimension, though (i) works for  $n - j \geq 3$ .

called Arnol'd relation [Arn]. Since Arnol'd relation is a natural assumption imposed on the graph complex of Arone and Turchin, this vanishing argument also highlights the similarity mentioned earlier. Note that one can refer [CCTW] for the computation of the 2-loop part of Arone and Turchin's graph homology.

The paper is organized as follows. First, in Section 1, we review recent works on the space  $\text{Emb}(\mathbb{R}^n, \mathbb{R}^{n+2})$  and configuration space integral associated with BCR graphs. After that, some definitions and notations are given in Section 2. Main Result is stated in Section 3. Then in Section 4, we construct the well-defined cocycles of  $\text{Emb}(\mathbb{R}^n, \mathbb{R}^{n+2})$ . In Section 5, we construct the cycles from chord diagrams on directed lines. In Section 6, we show preliminary lemmas used in the proof of Main Result. In Section 7, we give proof of Main Result by pairing the cocycles and the cycles of Section 4 and 5, described by graph-diagram pairing. Finally, in Section 8, we introduce a modified BCR graph complex to get higher-order or higher-loop graph cocycles.

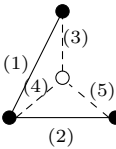
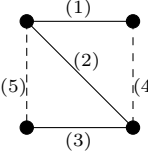
## Acknowledgement

The author is deeply grateful to his supervisor Mikio Furuta for his continuous support and encouragement for years. The author would like to thank Tadayuki Watanabe for teaching the author a lot about Watanabe's work. Discussion with Watanabe highly motivated the author during the preparation of this paper. The author thanks Keiichi Sakai for giving the author a great opportunity to talk and discuss at Shinshu Topology Seminar. Sakai also taught the author a lot about the space of embeddings. The author also thanks Masahito Yamazaki and Tatsuro Shimizu for helpful suggestions and stimulating conversations. The author thanks Victor Turchin for informing the author of the paper [FTW].

This research was supported by Forefront Physics and Mathematics Program to Drive Transformation (FoPM), a World-leading Innovative Graduate Study (WINGS) Program, the University of Tokyo.

## 1 Background

In this paper, we study the homotopy group and (co)homology of the space of

long embeddings by using graphs such as  and . As a

corollary of our main result, we give a non-trivial element of  $\pi_{n-1}(\text{Emb}_\partial(D^n, D^{n+2})_u)$  explicitly for  $n = 3$ . First, we introduce recent research on this group. See subsection 2.1 for the definition of the space  $\text{Emb}_\partial(D^n, D^{n+2})$ . This space is equivalent to  $\text{Emb}(\mathbb{R}^n, \mathbb{R}^{n+2})$ .

### 1.1 $\text{Emb}_\partial(D^n, D^{n+2})$ and $\text{Diff}_\partial(D^{n+1} \times S^1)$

We discuss the most important case  $n = 2$ , but other cases ( $n \geq 3$ ) run similarly. Let  $\text{Emb}_\partial(D^2, D^4)_u$  be the unknot component of  $\text{Emb}_\partial(D^2, D^4)$ . Budney-Gabai and Watanabe independently showed that  $\pi_1(\text{Emb}_\partial(D^2, D^4)_u)$  includes a subgroup of infinite rank.

**Theorem 1.1.** [BG] [Wat 6] Let

$$\text{Diff}_\partial(D^4) \rightarrow \text{Diff}_\partial(D^3 \times S^1) \rightarrow \text{Emb}_\partial(D^3, D^3 \times S^1)$$

be a fibration of Cerf and Palais [Cer][Pal]. Then

- $\pi_0(\text{Diff}_\partial(D^3 \times S^1)/\text{Diff}_\partial(D^4))$  has an infinite rank subgroup.
- $\pi_0(\text{Emb}_\partial(D^3, D^3 \times S^1)) \cong \pi_1(\text{Emb}_\partial(D^2, D^4)_u)$ .

Budney-Gabai has constructed elements of  $\text{Diff}_\partial(D^3 \times S^1)$  by the surgery along submanifolds which they call barbells. They have shown the non-triviality by introducing an invariant which Taylor approximation of  $\text{Emb}_\partial(D^1, D^3 \times S^1)$  induces. This approximation was developed by Goodwillie, Klein and Weiss [GW][GKW][Wei] and its mapping space model by Sinha [Sin].

On the other hand, Watanabe constructed elements of  $\text{Diff}_\partial(D^3 \times S^1)$  by the family version of clasper surgery [Hab][GGP][Wat 3][Wat 5]. He developed Kontsevich characteristic classes of local coefficients [Kon][Wat 3][Wat 5] to show the non-triviality:

$$Z_\theta : \pi_1(\widetilde{\text{BDiff}_\partial(D^3 \times S^1)}) \rightarrow \bigwedge^3 \mathbb{C}[t^{\pm 1}]/\mathbb{Z}.$$

In a similar way,  $\pi_{n-1}(\text{Emb}_\partial(D^n, D^{n+2})_u)$  is proved to have an infinite-rank subgroup for  $n \geq 2$ .

### 1.2 BCR graph complex and the de Rham complex of $\text{Emb}(\mathbb{R}^j, \mathbb{R}^n)$

Sakai in [Sak 2] defined the BCR graph complex  $(\mathcal{D}_g^{k,l}, \delta)$  and constructed a linear map from this space to the de Rham complex of  $\text{Emb}(\mathbb{R}^j, \mathbb{R}^n)$  by configuration space integral. This correspondence gives a higher dimensional analog (in the sense  $j \geq 2$ ) of the correspondence developed by Cattaneo, Cotta-Ramusino and Longoni [CCL]. Refer to subsection 2.2 and 2.3 for the definition of BCR graph complex.

**Theorem 1.2.** [Sak 2, Theorem 1.2] Let  $k \geq 1, g \geq 0$ . Configuration space integral gives a linear map

$$I : \mathcal{D}_g^{k,l} \rightarrow \Omega_{dR}^{k(n-j-2)+(g-1)(j-1)+l}(\text{Emb}(\mathbb{R}^j, \mathbb{R}^n)).$$

Moreover, if one of

- $n - j \geq 2$  is even and  $g = 0$
- $n > j \geq 3$  are odd and  $g = 1$

is satisfied, the map  $I$  gives a cochain map.

Based on the above theorem, it is expected that we can obtain non-trivial cohomology classes of  $\text{Emb}(\mathbb{R}^j, \mathbb{R}^n)$  if the graph cohomology is non-trivial and the map on the cohomology level induced from  $I$  satisfies injectivity.

From this perspective, Sakai and Watanabe conducted further research on  $g = 1$  (and  $l = 0$ ) in [SW], where configuration space integral invariants are put together into the universal one. Their work is based on the theory of finite type invariants for ribbon  $n$ -knots developed by Habiro, Kanenobu and Shima [HKS].

**Theorem 1.3.** [SW, Theorem 1.1] Let  $(n, j, k)$  satisfy some conditions. Let  $\mathcal{A}_1^k$  be the quotient of  $\mathcal{D}_1^{*,0}$  by some relations (such as the STU relation of Jacobi diagrams). Then there exists a linear and injective map

$$\alpha : \mathcal{A}_1^k \rightarrow H_{(n-j-2)k}(\text{Emb}(\mathbb{R}^j, \mathbb{R}^n), \mathbb{R}).$$

In fact, the universal configuration space integral invariant  $z_k$  gives a closed  $(n - j - 2)k$  form, and detects the non-triviality of the above cycle.

**Remark 1.4.** We can observe above that when  $n - j = 2$  we have to use graphs with  $g \geq 2$  or  $l \geq 1$  to obtain cocycles of higher degree.

**Remark 1.5.** The case  $l \geq 1$  is out of the scope of this paper. For the case of Jacobi diagrams ( $j = 1$ ), There is some progress by Sakai [Sak 1][Sak 3]. In these works, other types of cycles are constructed based on the case  $l = 0$ . Hence in our case as well, first focusing on  $l = 0$  case might be better.

## 2 Definition

### 2.1 The space of long embeddings

We first define the space of long embeddings and related spaces.

**Definition 2.1.** A long embedding is an embedding  $\mathbb{R}^j \rightarrow \mathbb{R}^n$ , which is standard outside a disk in  $\mathbb{R}^j$ . A long embedding  $\mathbb{R}^n \rightarrow \mathbb{R}^{n+2}$  is called a long  $n$ -knot. We equip the space  $\text{Emb}(\mathbb{R}^j, \mathbb{R}^n)$  of long embeddings  $\mathbb{R}^j \rightarrow \mathbb{R}^n$  with the induced topology from the weak  $C^\infty$  topology. We define the space of long immersions  $\text{Imm}(\mathbb{R}^j, \mathbb{R}^n)$  similarly.

**Remark 2.2.** Budney showed in [Bud] that  $\text{Emb}(S^j, S^n) \simeq SO_{n+1} \times_{SO_{n-j}} \text{Emb}(\mathbb{R}^j, \mathbb{R}^n)$ . That is, the difference between the two spaces  $\text{Emb}(S^j, S^n)$  and  $\text{Emb}(\mathbb{R}^j, \mathbb{R}^n)$  is given by Stiefel manifold  $SO_{n+1}/SO_{n-j}$ , whose homotopy groups are well-studied.

**Remark 2.3.** In this paper we often consider  $\text{Emb}_\partial(D^j, D^n)$ , the space of embeddings  $D^j \rightarrow D^n$  which are standard near the boundary, instead of  $\text{Emb}(\mathbb{R}^j, \mathbb{R}^n)$ . The homotopy types of these two spaces are equivalent.

For technical reasons, sometimes we think of the space of embeddings modulo immersions.

**Definition 2.4.** We write  $\overline{\text{Emb}}(\mathbb{R}^j, \mathbb{R}^n)$  for the homotopy fiber of the inclusion

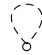
$$\text{Emb}(\mathbb{R}^j, \mathbb{R}^n) \hookrightarrow \text{Imm}(\mathbb{R}^j, \mathbb{R}^n)$$

at the standard inclusion  $\iota$ . That is, an element  $\{\phi_t\}$  of  $\overline{\text{Emb}}(\mathbb{R}^j, \mathbb{R}^n)$  is a one parameter family of long immersions which satisfies  $\phi_0 = \iota$ ,  $\phi_1 \in \text{Emb}(\mathbb{R}^j, \mathbb{R}^n)$ . Let  $r : \overline{\text{Emb}}(\mathbb{R}^j, \mathbb{R}^n) \rightarrow \text{Emb}(\mathbb{R}^j, \mathbb{R}^n)$  be a natural projection.

## 2.2 BCR graphs

We move on to the definition of BCR graphs and their complex. See Section 3 for examples of BCR graphs. Although we basically follow the definitions of [Bot][CR][Sak 2][SW][Wat 1], we restate them since there are some differences in formulations and conventions among these papers.

**Definition 2.5.** A BCR graph is a graph which satisfies the following conditions.



- (1) There are two types of vertices, white and black.
- (2) There are two types of edges, solid and dashed.
- (3) White vertices have only dashed edges, and their valency is more than three.
- (4) Black vertices have one or more dashed edges, with an arbitrary number of solid edges.
- (5) White vertices have no small loop. .
- (5) Black vertices have no small loops consisting of a solid edge alone.



(See Remark 2.7 below).

**Example 2.6.** Here are typical examples of vertices of BCR graphs.



**Remark 2.7.** Black vertices admit a small loop  and a double loop . We write the set of small loops of  $\Gamma$  as  $L_s(\Gamma)$  and the set of double loops as  $L_d(\Gamma)$ .  $L(\Gamma) = L_s(\Gamma) \sqcup L_d(\Gamma)$ .

**Notation 2.8.** Let  $\Gamma$  be a BCR graph. We denote the set of solid edges of  $\Gamma$  by  $E_\eta(\Gamma)$ , and the set of dashed edges by  $E_\theta(\Gamma)$ .

$$E(\Gamma) = E_\eta(\Gamma) \sqcup E_\theta(\Gamma).$$

We denote the set of black vertices of  $\Gamma$  by  $B(\Gamma)$ , and the set of white vertices by  $W(\Gamma)$ .

$$V(\Gamma) = B(\Gamma) \sqcup W(\Gamma).$$

**Definition 2.9** (Defect of a graph). Let  $v$  be a vertex of a BCR graph  $\Gamma$ . We define the defect  $l(v)$  of  $v$  as

$$l(v) = \begin{cases} \#E_\theta(v) - 3 & (v \in W(\Gamma)) \\ \#E_\theta(v) - 1 & (v \in B(\Gamma)). \end{cases}$$

The defect  $l(\Gamma)$  of  $\Gamma$  is defined as

$$l(\Gamma) = \sum_{v \in V(\Gamma)} l(v).$$

**Remark 2.10.** The defect of a graph measures how the graph is collapsed (or degenerate) compared to the standard ones, where each black vertex has exactly one dashed edge and each white vertex has exactly three dashed edges.

**Definition 2.11** (Order of a graph). The order  $k(\Gamma)$  of a BCR graph  $\Gamma$  is given by

$$k(\Gamma) = \#E_\theta(\Gamma) - \#W(\Gamma).$$

**Remark 2.12.** When the defect is 0, we have  $k = \frac{\#V(\Gamma)}{2}$ .

**Definition 2.13.** We give a color of  $\Gamma$  as follows.

- (1) When  $(n, j)$  is (odd, odd),  
a label of  $V(\Gamma)$ , an orientation of each  $e \in E(\Gamma)$  and a label of  $L_s(\Gamma)$ .
- (2) When  $(n, j)$  is (even, even),  
a label of  $V(\Gamma)$ , a label of  $E(\Gamma)$  and a label of  $L(\Gamma)$ .

In (1), we do not orient edges of small or double loops. In (2), the set  $E(\Gamma)$  includes one dashed edge for each small loop and includes one dashed edge and one solid edge for each double loop. A label of a set  $X$  with  $m$  elements is a bijective map from  $\{1, 2, \dots, m\}$  to  $X$ . We choose a label so that black vertices and solid edges are the first of labeling.



**Definition 2.14.** The orientation  $s$  of a colored graph  $\Gamma$  is determined by

- (1) when  $(n, j)$  is (odd, odd)

$$s \in \det \left( \mathbb{R}V(\Gamma) \bigoplus \bigoplus_{e \in E(\Gamma)} \mathbb{R}H(e) \right).$$

Here  $H(e)$  is the set of two vertices of  $e$ .

- (2) when  $(n, j)$  is (even, even)

$$s \in \det \left( \bigoplus \mathbb{R}E(\Gamma) \bigoplus \bigoplus \mathbb{R}L(\Gamma) \right).$$

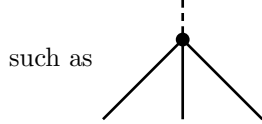
### 2.3 BCR graph complex

**Definition 2.15.** We define an equivalence relation of the vector space spanned by colored BCR graphs with order  $k$ , defect  $l$ . We denote the quotient space by  $\mathcal{D}^{k,l}$ .

- (1) Two colorings with the same orientation are identified, and those with opposite orientations are given opposite signs.
- (2)  $\Gamma = 0$  for any graph  $\Gamma$  with a double edge.



- (3) If  $n$  is odd,  $\Gamma = 0$  for any graph  $\Gamma$  with a double loop.
- (4) When  $l = 0$ , we set  $\Gamma = 0$  for any “non-admissible” graph  $\Gamma$ . A graph  $\Gamma$  is non-admissible if it has black vertices whose eta-valency is more than three



, or if it has a multiple edge



**Notation 2.16.** We write the subspace of  $\mathcal{D}^{k,l}$  generated by graphs with  $g$  loops as  $\mathcal{D}_g^{k,l}$ . (Here, we do not count small or double loops)

**Remark 2.17.** The fourth condition is just to make the computation of the top cohomology easier. So far, the author has yet to find precise reasons to exclude the possibility that we can construct a graph cocycle essentially using these non-admissible graphs. But one possible reason is that we can change non-admissible graphs to admissible graphs by Arnol’d relation (see subsection 2.4) with respect to solid edges.

**Remark 2.18.** One possible variant of  $\mathcal{D}$  is the graph complex  $\overline{\mathcal{D}}$  that is the same as  $\mathcal{D}$  for  $l \geq 0$  but has defect  $-1$  part  $\overline{\mathcal{D}}^{-1}$ . Here a graph with defect  $-1$  is a graph that has vertices of defect 0 and exactly one black vertex with three solid edges and no dashed edge. Contraction of the three solid edges adjacent to the black vertex yields Arnol’d relation.

Next, we define the coboundary operator  $\delta : \mathcal{D}_g^{k,l} \rightarrow \mathcal{D}_g^{k,l+1}$  of the graph complex.

**Definition 2.19** (Contraction of a BCR graph [Sak 2]). We define the contraction  $\Gamma/e$  of a BCR graph  $\Gamma$  at an edge  $e$  as follows.

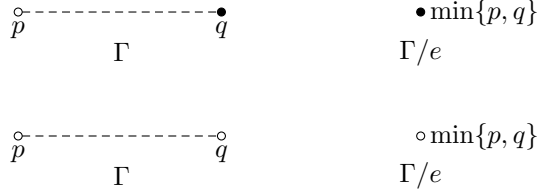
- (a) When  $e = (p, q) \in E_\eta(\Gamma)$  (except double edges).

Collapse  $e$  to the black vertex at the ends of  $e$  with a smaller label, and then reassign labels to edges and vertices of the collapsed graph in a natural way. (That is, assign  $\min\{p, q\}$  to this collapsed vertex, and subtract 1 from all vertex labels greater than  $\max\{p, q\}$ . In addition, if  $j$  (and  $n$ ) is even and  $e$  has label  $(i)$ , subtract 1 from all edge labels greater than  $i$ ).



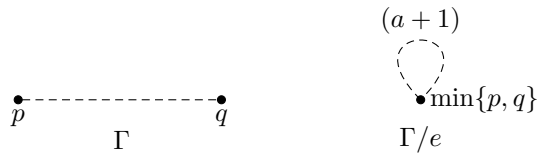
- (b) When  $e = (p, q) \in E_\theta(\Gamma)$  and at least one of  $p$  and  $q$  is white.

If exactly one is white, collapse  $e$  to the black vertex. If both are white, collapse  $e$  to the white vertex with a smaller label. The way to reassign labels is similar to (a).



- (c) When  $e = (p, q) \in E_\theta(\Gamma)$  and both  $p$  and  $q$  are black vertices.

We construct a small loop <sup>2</sup>. If the number of small and double loops of  $\Gamma$  is  $a$ , the label of this loop is  $(a + 1)$ .

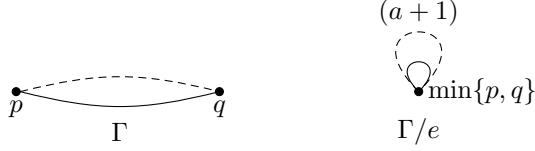


- (d) When  $e = (p, q)$  is the eta edge of a multiple edge.

We construct a double loop, and assign  $(a + 1)$  to this double loop.

---

<sup>2</sup>Though [Sak 2] introduces a kind of sign of small loop, it seems unnecessary.



**Definition 2.20** (Coboundary operator [Sak 2]). We define the coboundary operator  $\delta : \mathcal{D}_g^{k,l} \rightarrow \mathcal{D}_g^{k,l+1}$  of  $\mathcal{D}_g^{k,l}$  as follows:

$$\delta(\Gamma) = \sum_{e \in E(\Gamma) \setminus \{\text{loops}\}} \sigma(e) \Gamma/e.$$

Here, the sign  $\sigma(e)$  of an edge  $e$  is defined as follows.

- (1) When  $(n, j) = (\text{odd}, \text{odd})$ .

$$\sigma(e = (p, q)) = \begin{cases} (-1)^q & \text{if } p < q \\ (-1)^{p+1} & \text{if } p > q. \end{cases}$$

- (2) When  $(n, j) = (\text{even}, \text{even})$ .

$$\sigma(e) = \begin{cases} \sigma(e) = (-1)^i & \text{(If } e \text{ is type (a) or type (b) of Definition 2.19)} \\ \sigma(e) = (-1)^{a+1} & \text{(If } e \text{ is type (c) of Definition 2.19).} \end{cases}$$

Here  $i$  is the label of  $e$ , and  $a$  is the sum of the number of small and double loops. For multiple edges (type (d)), we consider that the edge is contracted and  $\sigma(e) = (-1)^{a+1}$ .

**Proposition 2.21.**  $(\mathcal{D}_g^{k,*}, \delta)$  is a cochain complex.

*Proof.* This follows from the fact that reversing the order of two contractions changes the sign.  $\square$

## 2.4 Comparing with Arone-Turchin graph complex

Arone and Turchin in [AT1] [AT2] defined two graph complexes  $\mathcal{E}^{m,n}$  and  $HH^{m,n}$  ( $m$  and  $n$  come from  $\text{Emb}(\mathbb{R}^m, \mathbb{R}^n)$ ). These complexes both arise from rather homotopy theoretical approaches: the description of the space of embeddings as a space of derived maps between modules over an operad.

$\mathcal{E}^{m,n}$  consists of so-called hairy graphs with two types of vertices. Graphs of  $HH^{m,n}$  have two types of edges as graphs of  $\mathcal{D}$ . The differences between  $HH^{m,n}$  and our complex  $\mathcal{D} = \mathcal{D}^{m,n}$  are

- 1 Their graph has only black vertices.
- 2 Their graph does not have solid or dashed loops (See Section 8).

- 3 Their contraction is performed only on solid edges.
- 4 Their complex is quotiented by another relation called Arnol'd relation as follows (two edges must be the same type).

$$\begin{array}{c}
 \begin{array}{ccc}
 \bullet & & \bullet \\
 \downarrow & & \downarrow \\
 i & \xrightarrow{1} & j \\
 \uparrow & & \uparrow \\
 \bullet & & \bullet \\
 & \nwarrow 2 & \nearrow 1 \\
 & k & 
 \end{array}
 + 
 \begin{array}{ccc}
 \bullet & & \bullet \\
 \downarrow & & \downarrow \\
 i & \xrightarrow{2} & k \\
 \uparrow & & \uparrow \\
 \bullet & & \bullet \\
 & \nwarrow 1 & \nearrow 2 \\
 & j & 
 \end{array}
 + 
 \begin{array}{ccc}
 \bullet & & \bullet \\
 \downarrow & & \downarrow \\
 i & \xrightarrow{1} & k \\
 \uparrow & & \uparrow \\
 \bullet & & \bullet \\
 & \nwarrow 2 & \nearrow 1 \\
 & j & 
 \end{array}
 = 0
 \end{array}$$

Note that conventions for solid and dashed edges are opposite from [AT1] and [AT2]: we follow the convention that solid edges correspond to  $\mathbb{R}^m$  of the domain.

## 2.5 Configuration space integral

From now on, for simplicity, we assume that graphs used to define configuration space integral are connected and satisfy  $l = 0$ , though these assumptions are not necessary if you just define the integral.

**Notation 2.22.** We write  $C_s(\mathbb{R}^n)$  for the configuration space of  $s$  points in  $\mathbb{R}^n$ :

$$C_s(\mathbb{R}^n) = (\mathbb{R}^n)^s \setminus \text{all diagonals}.$$

**Definition 2.23** (Configuration space). Let  $K : \mathbb{R}^j \hookrightarrow \mathbb{R}^n$  be a long embedding. Then we define the configuration space  $C_{s,t}(K, \mathbb{R}^n)$  as follows.

$$C_{s,t}(K, \mathbb{R}^n) = \{ (x_1, x_2, \dots, x_s, x_{s+1}, \dots, x_{s+t}) \in (\mathbb{R}^n)^{s+t} \setminus \text{all diagonals} \mid \forall i \in \{1, \dots, s\}, x_i \in K \}.$$

Hence  $C_{s,t}(K, \mathbb{R}^n)$  is the pullback of the following diagram.

$$\begin{array}{ccc}
 C_{s,t}(K, \mathbb{R}^n) & \longrightarrow & C_{s+t}(\mathbb{R}^n) \\
 \downarrow & & \downarrow \text{restriction} \\
 C_s(\mathbb{R}^j) & \xrightarrow{K \times n} & C_s(\mathbb{R}^n)
 \end{array}$$

**Definition 2.24** (Direction map). Let  $\Gamma$  be a colored BCR graph and  $s = \#B(\Gamma), t = \#W(\Gamma)$ . Let  $e = (i, j)$  be an edge of  $\Gamma$ . Here when  $(n, j) = (\text{even}, \text{even})$ , we arbitrary orient  $e$ , which does not affect the value of the integral defined later. Depending on  $e \in E_\theta(\Gamma)$  or  $e \in E_\eta(\Gamma)$ , the direction map  $\phi_e = \phi_{ij}$  from  $C_{s,t}(K, \mathbb{R}^n)$  to a sphere is defined as follows:

- If  $e = (i, j) \in E_\theta(\Gamma)$ ,

$$\phi_{ij} : C_{s,t}(K, \mathbb{R}^n) \longrightarrow C_2(\mathbb{R}^n) = C_{0,2}(\emptyset, \mathbb{R}^n) \longrightarrow S^{n-1}.$$

- If  $e = (i, j) \in E_\eta(\Gamma)$ ,

$$\phi_{ij} : C_{s,t}(K, \mathbb{R}^n) \longrightarrow C_2(\mathbb{R}^j) = C_{2,0}(K, \mathbb{R}^n) \longrightarrow S^{j-1}.$$

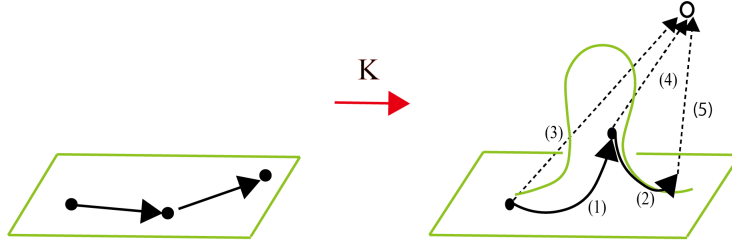
In both cases, the first map is the restriction

$$(x_1, x_2, \dots, x_s, x_{s+1}, \dots, x_{s+t}) \mapsto (x_i, x_j),$$

and the second is defined as

$$(x, y) \mapsto \frac{y - x}{\|y - x\|}.$$

Intuitively, dashed edges measure the direction between two points in  $\mathbb{R}^n$ , while solid edges measure the direction in  $\mathbb{R}^j$ .



**Definition 2.25** (Propagator). We define the differential form  $\omega(K, \Gamma)$  on  $C_{s,t}(K, \mathbb{R}^n)$  of degree  $(n-1)\#W(\Gamma) + (j-1)\#B(\Gamma)$  by

$$\omega(K, \Gamma) = \bigwedge_{e \in E_\eta(\Gamma)} \phi_e^* \omega_{S^{j-1}} \bigwedge_{e \in E_\theta(\Gamma)} \phi_e^* \omega_{S^{n-1}}.$$

Here, the order of the wedge product is given by the edge label.

**Remark 2.26.** The forms  $\phi_e^* \omega_{S^{j-1}}$  and  $\phi_e^* \omega_{S^{n-1}}$  are often called propagators. Leturcq [Let] has given more flexible propagators to define invariants of embeddings in rational homology  $n$ -spheres. The concept of admissible propagators was first introduced in [Les 2].

The next proposition ensures the convergence of the integral we later define.

**Proposition 2.27** (Existence of compactification). [AS][BT, Proposition 1.2] There exists a canonical compactification  $\overline{C}_{s,t}(K, \mathbb{R}^n)$  of  $C_{s,t}(K, \mathbb{R}^n)$  such that  $\phi_{ij}$  can be extended to the whole  $\overline{C}_{s,t}(K, \mathbb{R}^n)$ . The codimension 1 part of  $\partial \overline{C}_{s,t}(K, \mathbb{R}^n)$  is

$$\bigsqcup_{A \subset \{1, \dots, s, s+1, \dots, s+t, \infty\}} C_A,$$

where  $C_A$  is “the configuration space with  $A$  being infinitely close”. (See subsection 4.3 for details.)

**Definition 2.28.** We classify  $C_A$  ( $A \subset \{1, \dots, s, s+1, \dots, s+t, \infty\}$ ) into four types as follows ( $\Gamma_A$  is the subgraph of  $\Gamma$  generated by vertices of  $A$ ).

- Infinite faces:  $\infty \in A$ .
- Principal faces:  $|A| = 2$ .
- Hidden faces:  $|A| \geq 3$  and  $\Gamma_A$  is not the whole  $\Gamma$ .
- Anomalous faces:  $|A| \geq 3$  and  $\Gamma_A$  is the whole  $\Gamma$ .

**Definition 2.29** (Configuration space integral). Let  $\overline{C}_{s,t}(K, \mathbb{R}^n)$  be a typical fiber of the bundle  $\pi : \overline{C}_{s,t}(\mathbb{R}^n) \rightarrow \text{Emb}(\mathbb{R}^j, \mathbb{R}^n)$ . Let  $\Gamma$  be a colored BCR graph. We define configuration space integral associated with  $\Gamma$  by the fiber integral

$$I(\Gamma) = \int_{\overline{C}_{s,t}(K, \mathbb{R}^n)} \omega(\Gamma) = \int_{C_{s,t}(K, \mathbb{R}^n)} \omega(\Gamma).$$

The form  $I(\Gamma)$  on  $\text{Emb}(\mathbb{R}^j, \mathbb{R}^n)$  is also written as  $\pi_* \omega(\Gamma)$ .

By Stokes theorem [BT, Appendix][Wat 1, Appendix A.2] we have

$$\begin{aligned} dI(\Gamma) &= \pi_* \omega(\Gamma) + (-1)^r \pi_* \partial \omega(\Gamma) \\ &= \int_{\overline{C}_{s,t}(K, \mathbb{R}^n)} d\omega(\Gamma) + (-1)^r \int_{\partial \overline{C}_{s,t}(K, \mathbb{R}^n)} \omega(\Gamma) \\ &= (-1)^r \int_{\partial \overline{C}_{s,t}(K, \mathbb{R}^n)} \omega(\Gamma), \end{aligned}$$

where  $r$  is the degree of  $\int_{\partial \overline{C}_{s,t}(K, \mathbb{R}^n)} \omega(\Gamma)$ . Hence for the closedness of  $I(\Gamma)$ , we should check that the integral over each  $C_A$  vanishes. As usual, the contribution of infinite faces vanishes by dimensional reason. (Remember that all our embeddings are standard outside a disk.) On the other hand, we can cancel the contribution of principal faces of graphs by taking a graph cocycle.

### 3 Main Result

**Theorem 3.1.** Let  $(n, j) = (\text{odd}, \text{odd})$  with  $j \geq 3$ .

- 1 . The linear combination of 2-loop BCR graphs of order 3

$$H_2 = \sum_{i=1}^{21} w(\Gamma_i) \Gamma_i$$

is a graph cocycle. For the definition of  $\Gamma_i$  and its coefficient  $w(\Gamma_i)$ , see Figure 1.

2 . For the correction term  $\bar{c}(H_2)$  defined in Definition 4.6,

$$\bar{z}_2^3 = r^* I(H_2) + \bar{c}(H_2) \in \Omega_{dR}^{3n-2j-7} \overline{\text{Emb}}(\mathbb{R}^j, \mathbb{R}^n)$$

is closed and  $[\bar{z}_2^3] \in H_{dR}^{3n-2j-7} \overline{\text{Emb}}(\mathbb{R}^j, \mathbb{R}^n)$  is non-trivial. In fact we can explicitly construct  $\psi \in H_{3n-2j-7} \text{Emb}(\mathbb{R}^j, \mathbb{R}^n)$  and its lift  $\bar{\psi}$ , so that the pairing  $\bar{z}_2^3(\bar{\psi})$  is non-trivial. See Figure 7 for  $\psi$ .

3 . Moreover, if  $H_{dR}^{3n-j-6}(V_{n,j}(\mathbb{R})) = 0$ , we can obtain a non-trivial element  $z_2^3 \in H_{dR}^{3n-2j-7}(\text{Emb}(\mathbb{R}^j, \mathbb{R}^n))$ .

**Remark 3.2.** (See [MT, Theorem 3.14]) When  $(n, j) = (\text{odd}, \text{odd})$

$$H_{dR}^*(V_{n,j}) \cong \bigwedge (e_{n-j}, e_{2(n-j)+3}, e_{2(n-j)+7}, \dots, e_{2(n-j)+2j-3}).$$

In particular if  $j = 3$ ,  $H_{dR}^{3n-j-6}(V_{n,j}(\mathbb{R})) = 0$  holds.

**Remark 3.3.** A similar graph to the first graph  $\Gamma_1$  of Figure 1 appears in [AT2, Table C] as one of the rational homology generators of  $\mathcal{E}_\pi^{m,n}$ , the graph complex of hairy graphs. One can also check that  $HH_\pi^{m,n}$  has the last graph as one of the rational generators.

We can take the above non-trivial cycle  $\psi$  from the unknot component, and also over 2-sphere when the codimension is 2.

**Corollary 3.4.**

$$\pi_2(\text{Emb}_\partial(D^3, D^5)_u) \otimes \mathbb{Q} \neq 0.$$

**Theorem 3.5.** Let  $(n, j) = (\text{even}, \text{even})$  with  $j \geq 2$ .

1 .

$$H_1 = \frac{1}{2} \begin{array}{c} \bullet \\ \diagup \quad \diagdown \\ \textcircled{\bullet} \quad \textcircled{\bullet} \\ \diagdown \quad \diagup \\ \bullet \end{array} + \frac{1}{2} \begin{array}{c} \bullet \quad \bullet \\ \text{---} \quad \text{---} \\ \diagdown \quad \diagup \\ \bullet \quad \bullet \end{array}$$

(1) (2) (3) (4) (5)

is a non-trivial graph cocycle.

2 . For the correction term  $\bar{c}(H_1)$  defined in Definition 4.6,

$$\bar{z}_2^2 = r^* I(H_1) + \bar{c}(H_1) \in \Omega_{dR}^{2n-j-5} \overline{\text{Emb}}(\mathbb{R}^j, \mathbb{R}^n)$$

is closed.

3 . If  $H_{dR}^{2n-4}(V_{n,j}(\mathbb{R})) = 0$ , we can obtain  $z_2^2 = I(H_1) \in H_{dR}^{2n-j-5}(\text{Emb}(\mathbb{R}^j, \mathbb{R}^n))$ .

**Remark 3.6.**  $z_2^2$  (and  $\bar{z}_2^2$ ) is likely to vanish, since each graph of  $H_1$  vanishes after Arnol'd relation.

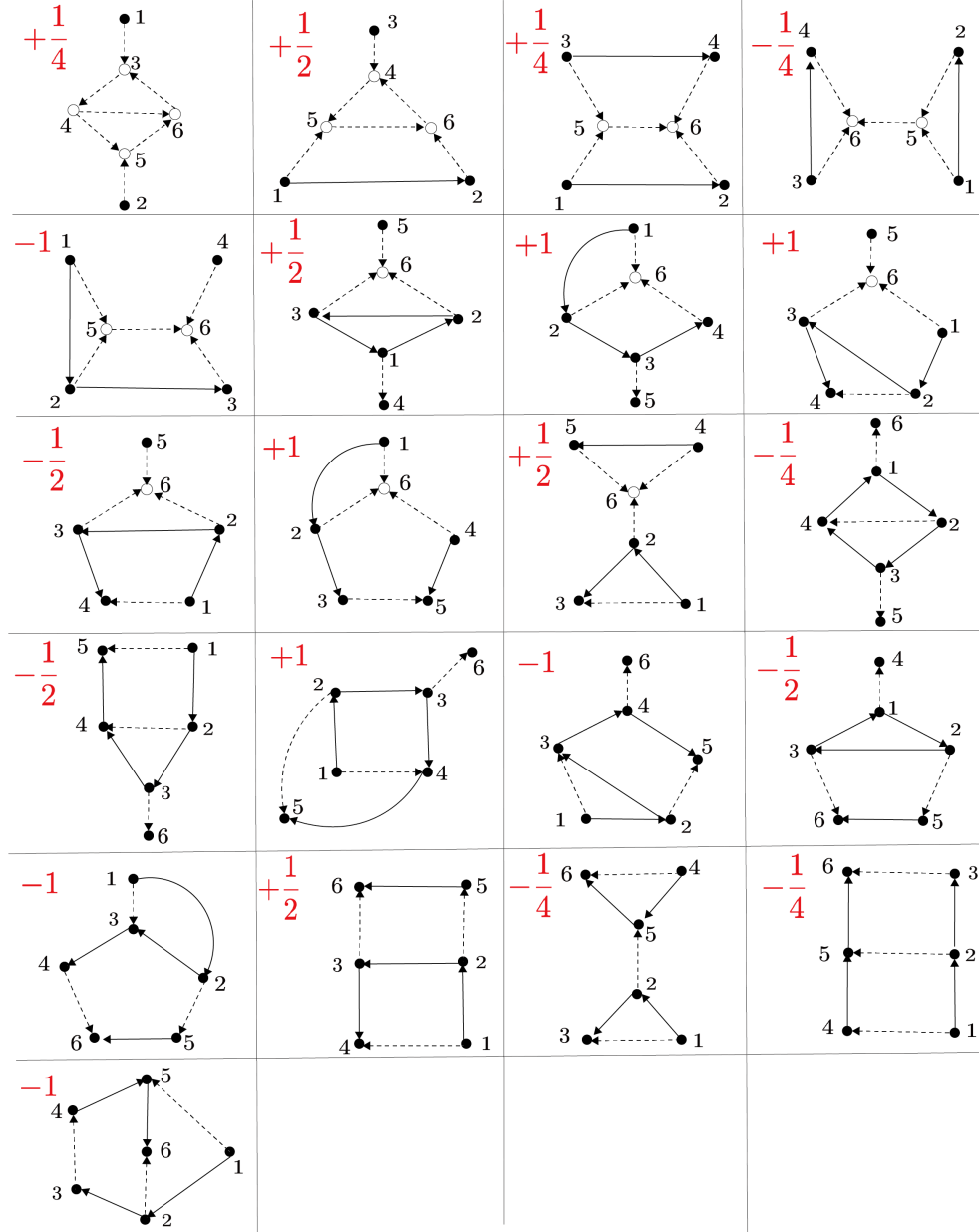


Figure 1: Non-trivial graph cocycle  $H_2$  (odd, odd)



$$\begin{aligned}
& \delta \begin{array}{c} \bullet \\ (1) \quad (3) \\ \diagdown \quad \diagup \\ \circ \\ (4) \quad (5) \\ \diagup \quad \diagdown \\ \bullet \quad \bullet \\ (2) \end{array} \\
= & - \begin{array}{c} \bullet \\ (2) \\ \diagdown \quad \diagup \\ \circ \\ (3) \quad (4) \\ \diagup \quad \diagdown \\ \bullet \quad \bullet \\ (1) \end{array} + \begin{array}{c} \bullet \\ (1) \\ \diagdown \quad \diagup \\ \circ \\ (3) \quad (4) \\ \diagup \quad \diagdown \\ \bullet \quad \bullet \\ (2) \end{array} - \begin{array}{c} \bullet \\ (1) \\ \diagdown \quad \diagup \\ \bullet \\ (3) \quad (4) \\ \diagup \quad \diagdown \\ \bullet \quad \bullet \\ (2) \end{array} + \begin{array}{c} \bullet \\ (1) \\ \diagdown \quad \diagup \\ \bullet \\ (3) \quad (4) \\ \diagup \quad \diagdown \\ \bullet \quad \bullet \\ (2) \end{array} - \begin{array}{c} \bullet \\ (1) \\ \diagdown \quad \diagup \\ \bullet \\ (4) \quad (3) \\ \diagup \quad \diagdown \\ \bullet \quad \bullet \\ (2) \end{array} \\
= & -2 \begin{array}{c} \bullet \\ (1) \\ \diagdown \quad \diagup \\ \bullet \\ (3) \quad (4) \\ \diagup \quad \diagdown \\ \bullet \quad \bullet \\ (2) \end{array} + \begin{array}{c} \bullet \\ (1) \\ \diagdown \quad \diagup \\ \bullet \\ (3) \quad (4) \\ \diagup \quad \diagdown \\ \bullet \quad \bullet \\ (2) \end{array} \\
& \delta \begin{array}{c} \bullet \\ (1) \\ \diagdown \quad \diagup \\ \bullet \\ (4) \quad (2) \quad (5) \\ \diagup \quad \diagdown \\ \bullet \quad \bullet \\ (3) \end{array} \\
= & - \begin{array}{c} \bullet \\ (4) \\ \diagdown \quad \diagup \\ \bullet \\ (3) \quad (1) \\ \diagup \quad \diagdown \\ \bullet \quad \bullet \\ (2) \end{array} + \begin{array}{c} \bullet \\ (1) \\ \diagdown \quad \diagup \\ \bullet \\ (3) \quad (4) \\ \diagup \quad \diagdown \\ \bullet \quad \bullet \\ (2) \end{array} - \begin{array}{c} \bullet \\ (1) \\ \diagdown \quad \diagup \\ \bullet \\ (3) \quad (2) \\ \diagup \quad \diagdown \\ \bullet \quad \bullet \\ (4) \end{array} + \begin{array}{c} \bullet \\ (4) \\ \diagdown \quad \diagup \\ \bullet \\ (3) \quad (1) \\ \diagup \quad \diagdown \\ \bullet \quad \bullet \\ (2) \end{array} + \begin{array}{c} \bullet \\ (1) \\ \diagdown \quad \diagup \\ \bullet \\ (4) \quad (2) \quad (5) \\ \diagup \quad \diagdown \\ \bullet \quad \bullet \\ (3) \end{array} \\
= & -2 \begin{array}{c} \bullet \\ (4) \\ \diagdown \quad \diagup \\ \bullet \\ (3) \quad (1) \\ \diagup \quad \diagdown \\ \bullet \quad \bullet \\ (2) \end{array} + \begin{array}{c} \bullet \\ (1) \\ \diagdown \quad \diagup \\ \bullet \\ (3) \quad (4) \\ \diagup \quad \diagdown \\ \bullet \quad \bullet \\ (2) \end{array}
\end{aligned}$$

Figure 2: Computation of  $\delta$  for  $H_1$

## 4 Construction of the cocycles

In this section, we show  $r^*I(H) + \bar{c}(H)$  is closed for  $H = H_1 \text{ or } H_2$ . According to the last paragraph of Section 2, what to show is vanishing of the contribution of principal, hidden and anomalous faces.

### 4.1 $H$ is a graph cocycle

We can show that  $H$  is a graph cocycle, by direct computation of the coboundary operator  $\delta$  defined in Definition 2.20. See Figure 2 for  $H_1$ . In this computation, it is necessary to put together isomorphic graphs with different colors, taking their orientations into account. This will be the most difficult part when computing the graph cohomology through computer calculus.

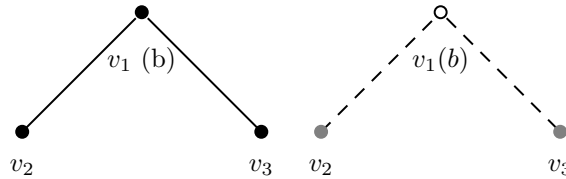
Note that for the top degree,  $\delta$  is described by a matrix (See Figure 3). We can easily see that the matrix is decomposed into blocks depending on the type of edges contracted: (A)  $\circ - - \circ$  (B)  $\bullet - - \bullet$  (C)  $\circ - - \bullet$  (D)  $\bullet \text{---} \bullet$ .

### 4.2 Vanishing of the contribution of hidden faces

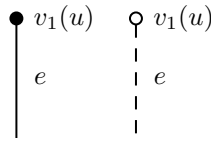
Here, we show that the contribution of hidden faces vanishes. For the graph cocycle  $H_1$  of Theorem 3.5, we apply the following proposition. The cancellation using the symmetry as below is first introduced by Kontsevich[Kon]. Lescop [Les 1][Les 3] gives a detailed explanation.

**Proposition 4.1.** Let  $s = \#B(\Gamma), t = \#W(\Gamma)$  and let  $C_A \subset \partial C_{s,t}(K, \mathbb{R}^n)$  be a hidden face. If the subgraph  $\Gamma_A$  of  $\Gamma$  satisfies one of the following conditions, the contribution of the integral over  $C_A$  vanishes. (Below  $u$  and  $b$  stand for univalent and bivalent, respectively).

- (1)  $\Gamma_A$  is not connected.
- (2)  $\Gamma_A$  has a bivalent vertex of the following form (gray vertices can be both black and white).



- (3)  $\Gamma_A$  has a univalent vertex of the following form.



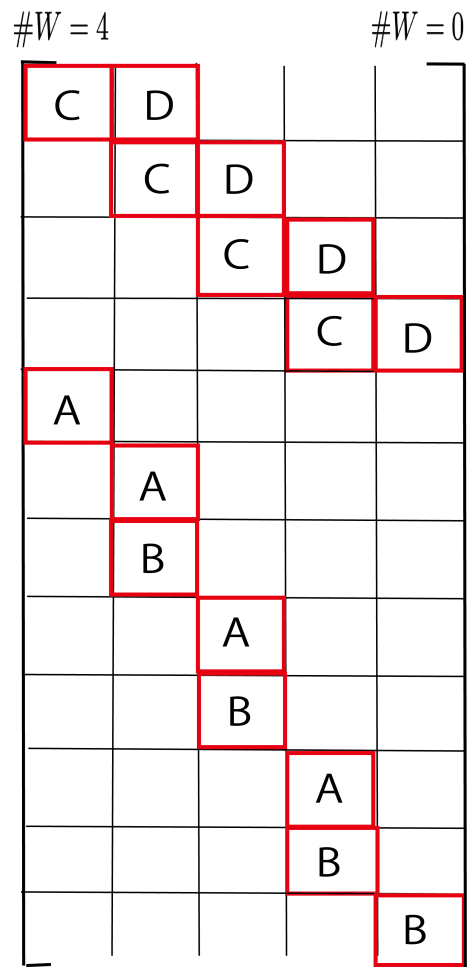


Figure 3: Coboundary operator  $\delta$

*Proof.* For (2), we use the involution of  $v_1$  with respect to the middle point of  $v_2$  and  $v_3$ :

$$v_1 \mapsto v_2 + v_3 - v_1.$$

When  $(n, j) = (\text{even}, \text{even})$ , this involution is orientation preserving, while the integrand form changes by  $(-1)$  due to the permutation of the two edges.

For (3), the group  $\mathbb{R}_+$  acts on  $C_A$  by rescaling the edge  $e$ . Since the form  $\omega(\Gamma)$  can be constructed through the projection

$$C_A \rightarrow C_A/\mathbb{R}_+,$$

where the quotient space on the right-hand side has less dimension, we can see the integral over  $C_A$  is zero.

For (1), we can use the action of  $\mathbb{R}_+$  that increases or decreases the distance of two components. □

We can easily see that all the hidden faces of  $H_1$  satisfy one of the above conditions. In the case of  $H_2$ , there exist hidden faces that do not satisfy any of the above conditions. However, since  $(n, j) = (\text{odd}, \text{odd})$  we can apply the following proposition that was shown in [Sak 2].

**Proposition 4.2.** • If  $n - j = \text{even}$  and  $\Gamma_A$  is 0-loop (a tree), the contribution of  $C_A$  vanishes.

• If  $(n, j) = (\text{odd}, \text{odd})$  and  $\Gamma_A$  is 1-loop, the contribution of  $C_A$  vanishes.

**Remark 4.3.** The second vanishing argument is also useful to cancel the contribution of the anomalous face, when  $(n, j) = (\text{odd}, \text{odd})$  and the number of loops is odd.

*Proof.* The first statement is a consequence of similar involutions and rescaling to those of Proposition 4.1. We review the involution used to prove the second statement. This is an involution of all the vertices of  $A$  with respect to one black vertex of  $A$

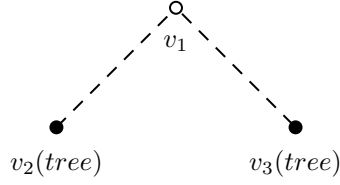
$$\begin{aligned} & (x_1, x_2, \dots, x_s, x_{s+1}, x_{s+2}, \dots, x_{s+t}) \\ \mapsto & (x_1, 2x_1 - x_2, \dots, 2x_1 - x_s, 2\iota(x_1) - x_{s+1}, 2\iota(x_1) - x_{s+2}, \dots, 2\iota(x_1) - x_{s+t}). \end{aligned}$$

□

If a subgraph  $\Gamma_A$  of  $\Gamma_i$  of the cocycle  $H_2$  is 2-loop, it satisfies one of (1) (2) (3). Hence, it follows that all the contributions of hidden faces of  $H_2$  do vanish.

**Remark 4.4.** Here, we list other involutions that will be useful to cancel the contribution of hidden faces of general BCR graphs.

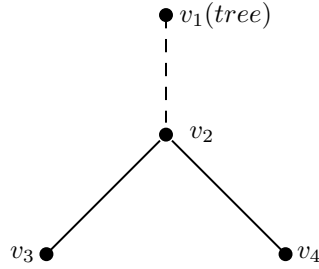
Case 1.  $(n - j = \text{even})$  When  $\Gamma_A$  has a pair of univalent vertices (or trees) of the following form.



Then the involution that exchanges  $v_2$  and  $v_3$  gives cancellation:

$$(v_2, v_3) \mapsto (v_3, v_2).$$

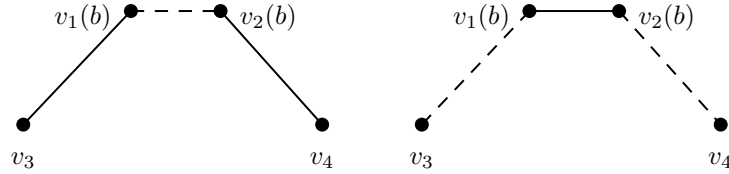
Case 2. When  $\Gamma_A$  has a univalent vertex (or a tree) of the following form.



After the involution of  $v_1$  with respect to  $v_2$ , perform that of  $v_1$  and  $v_2$  with respect to the middle point of  $v_3$  and  $v_4$

$$(v_1, v_2) \mapsto (v_1 + v_3 + v_4 - 2v_2, v_3 + v_4 - v_2).$$

Case 3. When  $\Gamma_A$  has a bivalent vertex of the following form



First exchange  $v_1$  and  $v_2$ , and perform the involution of  $v_1$  and  $v_2$  with respect to the middle point of  $v_3$  and  $v_4$

$$(v_1, v_2) \mapsto (v_3 + v_4 - v_2, v_3 + v_4 - v_1).$$

### 4.3 Construction of a correction term for anomalous faces

We now proceed to construct a correction term to cancel the contribution of the integral over the anomalous face  $C_{V(\Gamma)}$ . If  $H^*(V_{n,j}(\mathbb{R}))$  vanishes on a certain degree, we can construct a correction term  $c$  on  $\text{Emb}(\mathbb{R}^j, \mathbb{R}^n)$ . Otherwise we construct it on  $\overline{\text{Emb}}(\mathbb{R}^j, \mathbb{R}^n)$ , the space of embeddings modulo immersions.

Sakai in [Sak 2] takes the first approach, while Sakai and Watanabe do the second one in [SW].

For the above purpose, we first describe the structure of each codimension one face  $C_A$ . Readers can also refer to [Bot][CCL][Sak 2] for more detailed explanations. We only describe it when the subset  $A \subset V(\Gamma) = \{1, \dots, s, s+1, \dots, s+t\}$  has at least one element of  $\{1, \dots, s\}$ . The anomalous face is the case where  $A$  is equal to the entire  $V(\Gamma)$ .

The space  $C_A$  is defined as the pullback of the following diagram.

$$\begin{array}{ccc} C_A & \xrightarrow{\quad} & B_A \\ \downarrow & & \downarrow b \\ C_{V/A} & \xrightarrow{D} & \text{Inj}(\mathbb{R}^j, \mathbb{R}^n) \\ \downarrow \pi & & \\ \text{Emb}(\mathbb{R}^j, \mathbb{R}^n) & & \end{array}$$

Here,  $\text{Inj}(\mathbb{R}^j, \mathbb{R}^n)$  on the middle right is the space of linear injective maps from  $\mathbb{R}^j$  to  $\mathbb{R}^n$ .  $C_{V/A}$  on the middle left is the bundle over  $\text{Emb}(\mathbb{R}^j, \mathbb{R}^n)$  whose fiber is the configuration space of  $V(\Gamma)/A$ .  $B_A$  on the upper right is the bundle over  $\text{Inj}(\mathbb{R}^j, \mathbb{R}^n)$  with “normalized configuration space” of  $A$  as the fiber. More precisely, let

$$\begin{aligned} V(\Gamma)/A &= \{i_1, \dots, i_{s'}, i_{s'+1}, \dots, i_{s'+t'}\}, \\ A &= \{j_1, \dots, j_{s''}, j_{s''+1}, \dots, j_{s''+t''}\} \end{aligned}$$

( $s' + s'' = s + 1$ ). Then  $C_{V/A}(\psi)$  for each  $\psi$  in  $\text{Emb}(\mathbb{R}^j, \mathbb{R}^n)$  and  $B_A(I)$  for each  $I \in \text{Inj}(\mathbb{R}^j, \mathbb{R}^n)$  is defined as

$$\begin{aligned} C_{V/A}(\psi) &= C_{s', t'}(\psi) \quad (\psi \in \text{Emb}(\mathbb{R}^j, \mathbb{R}^n)) \\ B_A(I) &= C_{s'', t''}(I) / \sim \quad (I \in \text{Inj}(\mathbb{R}^j, \mathbb{R}^n)). \end{aligned}$$

Here,  $\sim$  is an equivalence relation generated by (a) rescaling (b) translations in  $I$  direction:

- (a)  $(x_{j_1}, \dots, x_{j_{s''}}, x_{j_{s''}+1}, \dots, x_{j_{s''}+j_{t''}}) \sim r(x_{j_1}, \dots, x_{j_{s''}}, x_{j_{s''}+1}, \dots, x_{j_{s''}+j_{t''}}) \quad (r \in \mathbb{R}_{>0})$
- (b)  $(x_{j_1}, \dots, x_{j_{s''}}, x_{j_{s''}+1}, \dots, x_{j_{s''}+j_{t''}}) \sim v + (x_{j_1}, \dots, x_{j_{s''}}, y_{j_{s''}+1}, \dots, x_{j_{s''}+j_{t''}}) \quad (v // I).$

$D$  in the above diagram is a map from  $C_{V/A}$  to  $\text{Inj}(\mathbb{R}^j, \mathbb{R}^n)$  which gives the differential of  $\psi$  at a collapsed point  $A/A$ .

**Proposition 4.5.** Let  $H = \sum_i \Gamma_i$  be a graph cocycle such that the contribution of hidden faces are canceled. For each  $\Gamma$  of  $H$ , set  $A = V(\Gamma)$  and consider the bundle  $b : B_A \rightarrow \text{Inj}(\mathbb{R}^j, \mathbb{R}^n)$ . Then the fiber integral

$$b_*\omega(H) = \sum_i b_*\omega(\Gamma_i) \in \Omega_{dR}^d(\text{Inj}(\mathbb{R}^j, \mathbb{R}^n)), \quad d = k(n-j-2) + (g-1)(j-1) + (j+1)$$

is closed. Moreover, when  $b_*\omega(H)$  is exact, we can construct a correction term of the anomalous face by using  $\mu \in \Omega_{dR}^{d-1}(\text{Inj}(\mathbb{R}^j, \mathbb{R}^n))$  which satisfies  $d\mu = (-1)^{r+1}b_*\omega(H)$  ( $r = d - j$ ):

$$c(H) = \pi_* D^* \mu.$$

*Proof.* Without loss of generality, assume  $H = \Gamma_1 + \Gamma_2$ . We show that  $I(H) + c(H)$  is closed.

$$\begin{aligned} (-1)^r dI(H) &= \int_{C_V(\Gamma_1)} \omega(\Gamma_1) + \int_{C_V(\Gamma_2)} \omega(\Gamma_2) \\ &= \pi_* D^* b_{1*} \omega(\Gamma_1) + \pi_* D^* b_{2*} \omega(\Gamma_2) \\ (-1)^r dc(H) &= (-1)^r d\pi_* D^* \mu \\ &= (-1)^r \pi_* D^* d\mu + \pi_*^\partial D^* \mu \\ &= -\pi_* D^* b_{1*} \omega(\Gamma_1) - \pi_* D^* b_{2*} \omega(\Gamma_2) \end{aligned}$$

□

Next, we consider the case  $H_{dR}^d(\text{Inj}(\mathbb{R}^j, \mathbb{R}^n)) = H_{dR}^d(V_{n,j}) = 0$  is not satisfied. In this case, we construct a correction term of  $r^*I(H) \in \Omega^{k(n-j-2)+(g-1)(j-1)}\overline{\text{Emb}}(\mathbb{R}^j, \mathbb{R}^n)$ . Define

$$\overline{D} : [0, 1] \times C_1(\mathbb{R}^j) \times \overline{\text{Emb}}(\mathbb{R}^j, \mathbb{R}^n) \longrightarrow \text{Inj}(\mathbb{R}^j, \mathbb{R}^n)$$

by  $\overline{D}(t, x, \overline{\phi}) = D(\overline{\phi}(t))_x$ . Note that  $\overline{D}(0) = D \circ (id \times r)$ .

**Definition 4.6.** We define the correction term for  $\Gamma$  by

$$\overline{c}(\Gamma) = (-1)^r (-1)^{d+1} \pi_* p_{23*} \overline{D}^* b_* \omega(\Gamma).$$

For a graph cocycle  $H = \sum_i \Gamma_i$ , set  $\overline{c}(H) = \sum_i \overline{c}(\Gamma_i)$ .

**Proposition 4.7.** Let  $H = \sum_i \Gamma_i$  be a graph cocycle such that the contributions of hidden faces are canceled. Then  $\overline{c}(H)$  defines the correction term of  $r^*I(H)$ .

*Proof.*

$$\begin{aligned} (-1)^r d\overline{c}(H) &= (-1)^{d+1} \pi_* d(p_{23*} \overline{D}^* b_{1*} \omega(\Gamma_1)) + (-1)^{d+1} \pi_* d(p_{23*} \overline{D}^* b_{2*} \omega(\Gamma_2)) \\ &= -\pi_* (id \times r)^* D^* b_{1*} \omega(\Gamma_1) - \pi_* (id \times r)^* D^* b_{2*} \omega(\Gamma_2) \\ &= -r^* \pi_* D^* b_{1*} \omega(\Gamma_1) - r^* \pi_* D^* b_{2*} \omega(\Gamma_2) \\ &= -\int_{C_V(\Gamma_1)} \omega(\Gamma_1) - \int_{C_V(\Gamma_2)} \omega(\Gamma_2). \end{aligned}$$

$$\begin{array}{ccccc}
\text{Emb}(\mathbb{R}^j, \mathbb{R}^n) & \xleftarrow{\pi} & C_1(\mathbb{R}^j) \times \text{Emb}(\mathbb{R}^j, \mathbb{R}^n) & & \\
\uparrow r & & \uparrow id \times r & \searrow D & \\
\overline{\text{Emb}}(\mathbb{R}^j, \mathbb{R}^n) & \xleftarrow{\pi} & C_1(\mathbb{R}^j) \times \overline{\text{Emb}}(\mathbb{R}^j, \mathbb{R}^n) & & \text{Inj}(\mathbb{R}^j, \mathbb{R}^n) \xleftarrow{b} B_V(\Gamma) \\
& & \uparrow p_{23} & \nearrow \overline{D} & \\
& & [0, 1] \times C_1(\mathbb{R}^j) \times \overline{\text{Emb}}(\mathbb{R}^j, \mathbb{R}^n) & & 
\end{array}$$

□

## 5 Construction of the cycles

We construct cycles of the space of long embeddings from what we call “a set of planetary systems” on  $\mathbb{R}^j$ . Furthermore, we will see that such a set of planetary systems is described by a chord diagram on directed lines.

### 5.1 Planetary systems and chord diagrams on directed lines

Using the terminology “planetary system” for configuration spaces appears in Sinha’s work [Sin2].

**Definition 5.1** (A set of planetary systems on  $\mathbb{R}^j$ ). A set of planetary systems  $\mathcal{S}$  on  $\mathbb{R}^j$  of order  $k$  consists of the following.

- (1) Points  $a_i$  at  $(i, 0, \dots, 0) \in \mathbb{R}^j$  ( $i = 1, \dots, s$ ).
- (2) Spheres  $S(L_i^j, a_i)$  ( $j = 1, \dots, t_i$ ) with radius  $L_i^j$  centered at  $a_i$  ( $i = 1, \dots, s$ ).  
Here sum of the number of points and spheres must be  $2k$ . We also assume  $L_i^j \ll 1$ , and assume if  $j < j'$ ,  $L_i^j \ll L_i^{j'}$ . For example, set  $\delta = \frac{1}{10^N}$  and  $L_i^j = \delta^{(t_i+1-j)}$ .

Below we call points of (1) fixed stars. We call spheres of (2) planetary orbits. Each fixed star forms one planetary system which consists of  $t_i$  planetary orbits.

**Definition 5.2** (Choice of pairings). A choice of (ordered) pairings  $\{p_i\}_{i=1, \dots, k}$  for  $\mathcal{S}$  is a pairing among the set of fixed stars and planetary orbits. Fixed stars must be paired with planetary orbits. Planetary orbits may be paired with other planetary orbits (orbit-orbit pairing). The order of two elements of each pair is taken so that the fixed star (if it exists) is the first.

A set of planetary systems and its ordered pairing can be described by a chord diagram on directed lines.

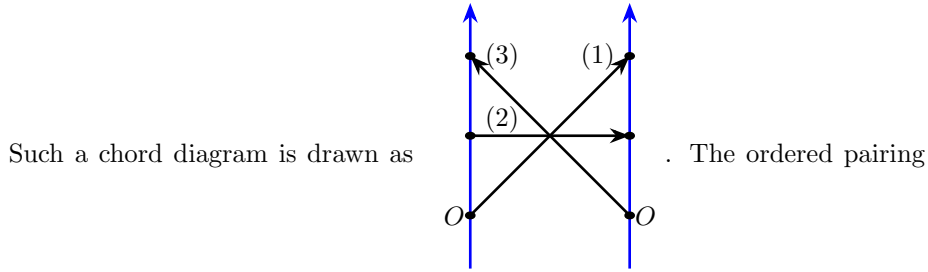


**Definition 5.3** (Chord diagram on directed lines). A chord diagram on  $s$  directed lines with order  $k$  consists of the following data.

- Integers  $t_i \geq 0$  ( $i = 1, \dots, s$ ) with

$$\sum_{i=1}^s (t_i + 1) = 2k.$$

- An ordered pairing  $\{p_i\}_{i=1, \dots, k}$  among  $2k$  points  $V = \{(i, j) \in \mathbb{Z}^2 | 1 \leq i \leq s, 0 \leq j \leq t_i\}$ .



- At least one of the two points of each pairing is off  $x$ -axis (that is, its second coordinate is not zero).
- Any point  $v = (i, 0)$  on  $x$ -axis must be the first of some ordered pairing.

A set of planetary systems and its ordered pairing determines a chord diagram on directed lines in an expected way. Namely, points on  $x$ -axis are fixed stars. Other points are planetary orbits. Conversely, a chord diagram on directed lines determines a set of planetary systems (up to some rescaling) and its ordered pairing.

Let  $C$  be a chord diagram on directed lines. Remember that the set of chords(pairings)  $E(C)$  is labeled by  $1, \dots, k$ , and each chord is oriented.

**Definition 5.4** (Induced labeling of  $V(C)$ ). We label the set of vertices  $V(C)$  in a canonical way using these ordering and orientation. That is, the initial vertex of  $i$ th chord is labeled by  $2i - 1$ . The end vertex of  $i$ th chord is labeled by  $2i$ .

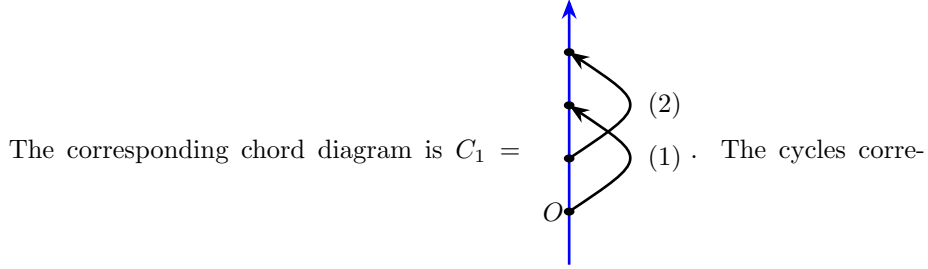
Using this labeling, let the image of  $\tau : \{1, \dots, g - 1\} \rightarrow \{1, \dots, 2k\}$  be the first vertex of some orbit-orbit pairing. Here,  $g - 1$  is the number of first vertices of orbit-orbit pairings. We assume that  $\tau$  preserves the orders.

## 5.2 Construction of the cycles

Once we fix a set of planetary systems and its ordered pairing, namely a chord diagram on directed lines, we can construct a “generalized ribbon cycle”. These generalized cycles have more parameters than “ribbon cycles” appeared in [SW], which they call “wheel-like cycles”.

**Definition 5.5** (Generalized ribbon cycles). Let  $\mathcal{S}$  be a set of planetary systems of order  $k$ . Let  $\{p_i\}_{i=1,\dots,k}$  be a choice of (ordered) pairings. Let  $g - 1$  be the number of orbit-orbit pairings. From this data, we construct  $k(n - j - 2) + (g - 1)(j - 1)$  cycle  $\psi = \psi(\mathcal{S}, \{p_i\}_{i=1,\dots,k})$  in the following. We call this cycle the generalized ribbon cycle associated with  $\mathcal{S}, \{p_i\}_{i=1,\dots,k}$ . For simplicity, we only construct for the following case:

- There is only one fixed star  $a_1$  (and hence one planetary system).
- There are three planetary orbits  $S(L_j, a_1)(j = 1, 2, 3)$ .
- The pairing is taken as  $(a_1, S(L_2)), (S(L_1), S(L_3))$ .



sponding to other  $(\mathcal{S}, \{p_i\}_{i=1,\dots,k})$  are constructed similarly.

Below we construct a cycle of  $\text{Emb}(\mathbb{R}^j, \mathbb{R}^n)$

$$\phi : S^{j-1} \times S^{n-j-2} \times S^{n-j-2} \rightarrow \text{Emb}(\mathbb{R}^j, \mathbb{R}^n).$$

This is one of the candidates for a dual cycle of  $H_1$ .

Let  $S(L)$  and  $D(L)$  denote  $(j - 1)$ -sphere and  $j$ -ball respectively, of radius  $L$  centered at  $O$  in  $\mathbb{R}^j$ . And let  $L_0, L_1, L_2, L_3 \in \mathbb{R}$  satisfy

$$L_0 \ll L_1 \ll L_2 \ll L_3.$$

(For example again, set  $L_i = \delta^{4-i}$ ). For each  $\theta \in S^{j-1}$ , we write  $D_\theta(\varepsilon)$  for the ball of radius  $\varepsilon$  centered at  $\theta \in S(L_1)$  ( $\varepsilon \ll L_1$ . For example,  $\varepsilon = \delta^4$ ) (See Figure 4). Step 1 and Step 2 below are to construct a cycle  $\phi_\theta : S^{n-j-2} \times S^{n-j-2} \rightarrow \text{Emb}(\mathbb{R}^j, \mathbb{R}^n)$  for each parameter  $\theta \in S^{j-1}$ . Let  $0 < h_0 < h_1 < h_2 < h_3 < h_4$  be coordinates of  $x_{j+1}$  axis.

Step 1 : Deform  $D(L_3)$  by isotopy in  $\mathbb{R}^j \times \mathbb{R} \subset \mathbb{R}^n$  to  $x_{j+1}$  direction, so that  $\mathbb{R}^j$  is embedded in  $\mathbb{R}^{j+1}$  as

$$S(r) \times (h_4, h_0) \quad (r \ll \min\{|h_i - h_{i+1}|\}_i)$$

in the range  $h_0 > x_{j+1} > h_4$ . Here  $S(L_3)$ ,  $S(L_2)$  and  $S(L_1)$  is mapped to  $S(r) \times \{h_3\}$ ,  $S(r) \times \{h_2\}$  and  $S(r) \times \{h_1\}$  respectively.

Step 2 : For  $L = L_2, L_3$ , let  $S(L) \times I$  be the tubular neighborhood of  $S(L)$  in  $\mathbb{R}^j$  with width  $2\varepsilon$ . Construct a ribbon link of  $S(L_3) \times I$  and  $D_\theta(\varepsilon)$  near

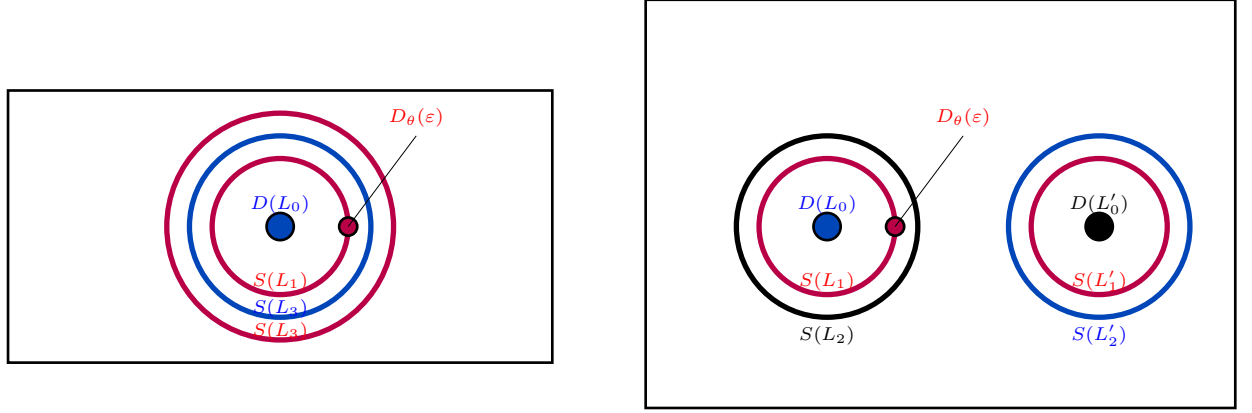


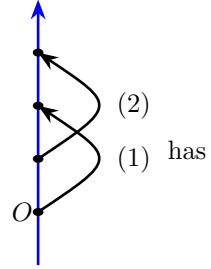
Figure 4: Preimage on  $\mathbb{R}^j$  of  $\phi$ (left) and  $\psi$ (right)

$S(r) \times h_3$ , and that of  $S(L_2) \times I$  and  $D(L_0)$  near  $S(r) \times h_2$ . (The ribbon links are constructed from the perturbation of ribbon presentations as in subsection 5.3). See Figure 5. Then we obtain a cycle

$$\phi_\theta : S^{n-j-2} \times S^{n-j-2} \rightarrow \text{Emb}(\mathbb{R}^j, \mathbb{R}^n).$$

By choosing a ribbon presentation suitably, we can construct this cycle in

the unknot component. Here we use the fact that  $C_1 =$



a specific subdiagram. See subsection 5.3.

Step 3 : Move  $\theta$  on  $S(L_1)$ . In  $\mathbb{R}^{n+1}$ , we change the behavior only near  $h_1$ . At the height  $h_1$ , we turn the branch tube around the stem tube. See Figure 5. Then we get the desired cycle  $\phi$ . (Figure 5.)

We describe Step 3 more precisely. We denote  $S^{j-1}(r) \times (h_4, h_0)$  as  $U$ . In Figure 5, we draw the core of  $U$  in blue, which is also denoted by  $U$ . For  $\theta$  in  $S^{j-1} \subset \mathbb{R}^j$ , let  $\partial D_\theta(\varepsilon)$  be mapped to  $\theta$  side of  $U$ .

For the initial point  $O = (L_1, 0, \dots, 0) \in S(L_1)$ , by deforming  $D_O(\varepsilon)$  by isotopy to  $x_1$ -direction, we construct near  $h_2$  a tube  $T$  with small radius which starts from  $U$ . We draw the core of  $T$  in red, also written as  $T$ .

At parameter  $\theta \in S^{j-1}$ ,  $T$  has the following form near  $h_1$  :

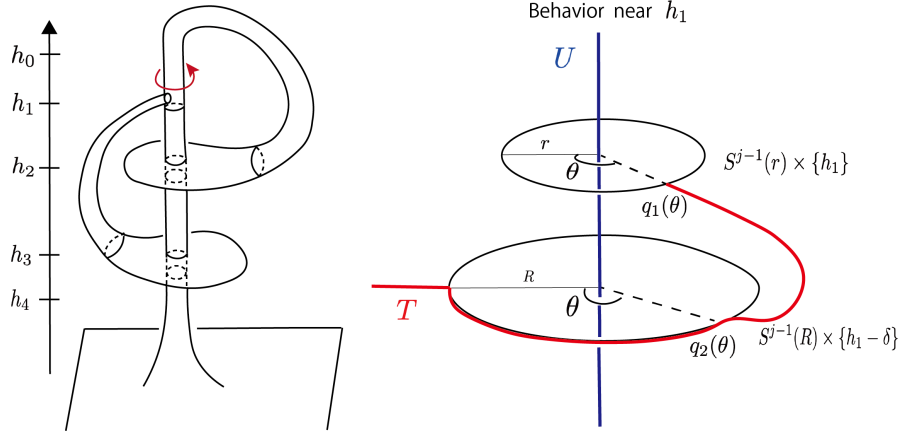


Figure 5: Image on  $\mathbb{R}^{j+1}$

- $T$  starts from  $U$  at  $q_1(\theta) = (r\theta, h_1) \in S^{j-1}(r) \times \{h_1\}$  and goes straight to  $(R\theta, h_1) \in S^{j-1}(R) \times \{h_1\}$  ( $R > r$ ).
- Next  $T$  runs down to  $S^{j-1}(R) \times \{h_1 - \delta\}$  preserving  $\theta \in S^{j-1}(R)$  and touches  $q_2(\theta) = (R\theta, h_1 - \delta)$ .
- Then  $T$  connects  $q_2(\theta)$  and  $q_2(O)$  through the shortest geodesic of  $S^{j-1}(R)$ .

However, there is one problem. When  $\theta$  is the antipode  $A$  of the base point  $O$ , there are infinitely many geodesics from  $q_2(A)$  to  $q_2(O)$ . To avoid this, we take a short-cut from  $q_2(\theta)$  to  $q_2(O)$  through the ball  $D^j(R)$  when  $\theta$  is near  $A$ . At the same time, when  $\theta$  is near  $A$ , we perturb the family of embeddings to  $x_{j+2}$ -direction.

More precisely, we regard the parameter space  $S^{j-1}$  as the ball of diameter 1 with its boundary identified. For  $v \in S^{j-1}$ ,  $\|v\|$  means the distance from the boundary to  $v$ . We assume that in the range  $\|v\| > 0.45$ , the core of  $T$  approaches the core of  $U$ , and that they intersect in  $\mathbb{R}^{j+1}$  when  $\|v\| = 0.5$ . At that time, we perturb  $T$  in the positive direction of  $x_{j+2}$  axis. See Figure 6.

This concludes the construction of  $\phi$ . As for  $H_2$ , we construct the generalized

ribbon cycle in Figure 7 from . In general, cycles have parameter  $\theta'_i \in S^{j-1}$  ( $i = 1, \dots, g-1$ ) and  $y_j \in S^{n-j-2}$  ( $j = 1, \dots, k$ ).

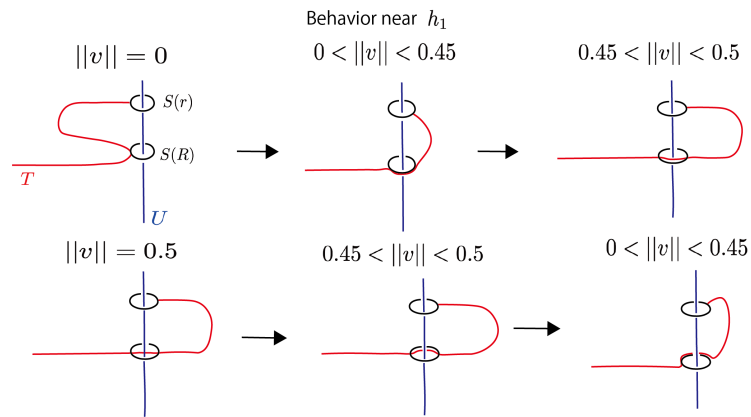


Figure 6: Perturbing to  $x_{j+2}$ -direction

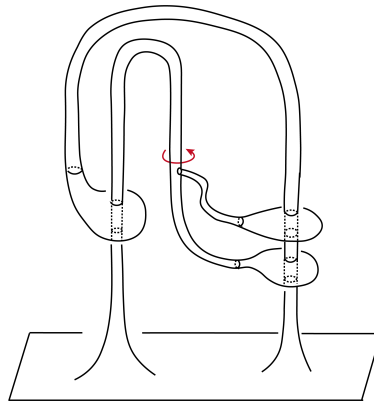


Figure 7: Cycle  $\psi$

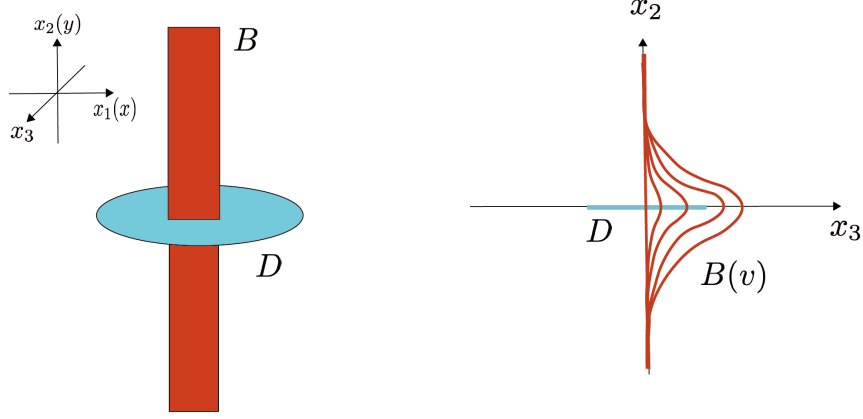


Figure 8: Perturbation of a ribbon presentation

### 5.3 Perturbation of ribbon presentations

Here, we describe the perturbation of ribbon presentations. Although the content of this subsection is a repetition of [Wat 1][SW], we also discuss suitable ribbon presentations to make the cycle of subsection 5.2 in the unknot component.

Let

$$B = \{(x_1, x_2, x_3) \in \mathbb{R}^3 \mid |x_1| \leq \frac{1}{2}, x_3 = 0\}$$

$$D = \{(x_1, x_2, x_3) \in \mathbb{R}^3 \mid |x_1|^2 + |x_3|^2 \leq 1, x_2 = 0\},$$

where  $B$  and  $D$  stand for Band and Disk, respectively. And let

$$S = S^{n-j-2} = \{(0, 0, x_3, \dots, x_{n-j+1}) \in \mathbb{R}^{n-j+1} \mid (x_3 - 1)^2 + x_4^2 + \dots + x_{n-j+1}^2 = 1\}.$$

Note that if  $n - j - 2 = 0$ ,  $S$  is two points  $S^0$ . The band obtained by perturbing  $B$  to  $v \in S$  direction is written as  $B(v)$  (Figure 8):

$$B(v) = \left\{ \{(x, y, \gamma(y)v) \in \mathbb{R}^2 \times \mathbb{R}^{n-j-1} \mid |x| \leq \frac{1}{2}\} \right\}.$$

Here  $\gamma(y)$  is a smooth function defined as

$$\gamma(y) = \begin{cases} \exp(-y^2/\sqrt{9-y^2}) & (|y| \leq 3) \\ 0 & (|y| \geq 3) \end{cases}.$$

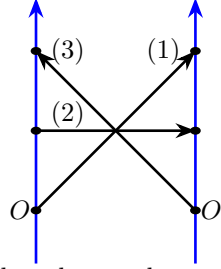
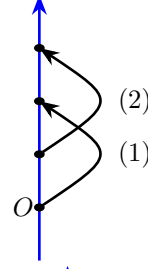
The ribbon link  $T(v) \cup S$  is constructed from  $P(v) = B(v) \cup D$  ( $v \in S^{n-j-2}$ ) as follows.

$$T(v) = \partial(B(v) \times [-1, 1]^{j-1})$$

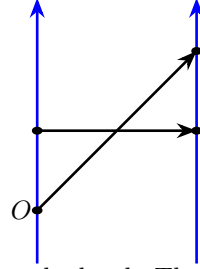
$$S = \partial(D \times [-2, 2]^{j-1}).$$

Next, we see how to construct a ribbon presentation that yields a cycle of

trivial long embeddings. Observe that our chord diagrams  $C_1 =$

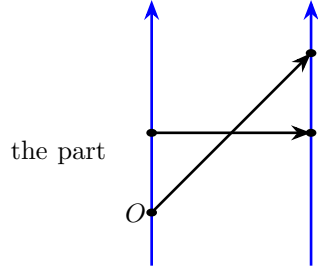


have a subdiagram of the form



. Remember

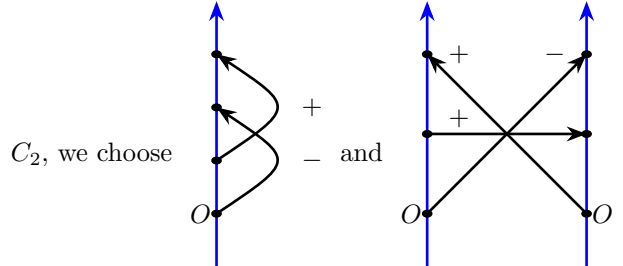
that we have constructed a ribbon crossing for each chord. There are two choices for each chord depending on which way the band crosses the disk. In



the part

, we take the left presentation of Figure 9. That is,

we assume that two crossings are of opposite sign. We can write this crossing information on chord diagrams by assigning a sign to each chord. For  $C_1$  and



$C_2$ , we choose

+

- and

.

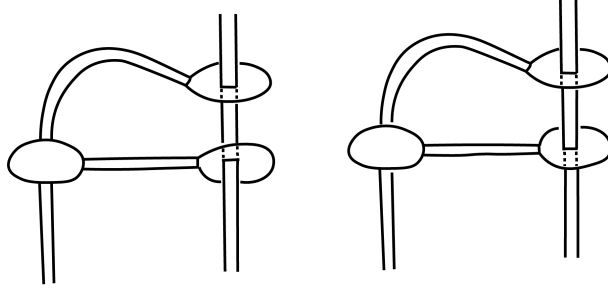


Figure 9: Suitable ribbon presentation (left)

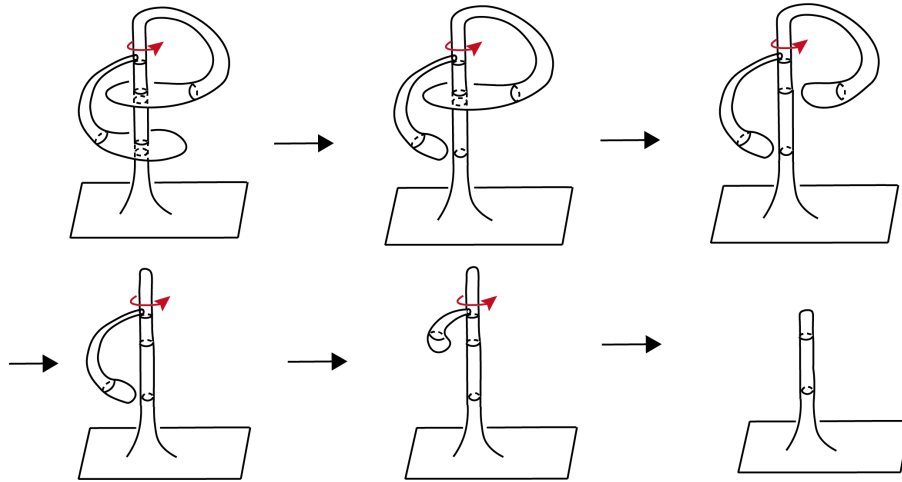


Figure 10: Lift of  $\phi$  to  $\overline{\text{Emb}}(\mathbb{R}^j, \mathbb{R}^n)$

#### 5.4 Lifting the cycles to $\overline{\text{Emb}}(\mathbb{R}^j, \mathbb{R}^n)$

By resolving ribbon links in order, which is possible through immersion, we can give a 1-parameter family from the given cycle to the trivial cycle of trivial long embeddings (Figure 10).

## 6 Some lemmas for computing cocycle-cycle pairing

In this section, we state fundamental lemmas which are used to calculate pairings between cocycles and cycles of the space of embeddings as pairings between graphs and diagrams (See Lemma 6.13). Readers who are familiar with con-



figuration space integral may skip until Lemma 6.7. Graphs in this section are admissible (See Definition 2.15) graphs with defect 0.

**Lemma 6.1** (Symmetry lemma). Let a colored graph  $\Gamma$  have an even symmetry  $\iota$  (a change of colors of even sign that produces the same colored graph). Consider the involution on  $C_{s,t}$

$$\sigma : (x_1, x_2, \dots, x_s, x_{s+1}, \dots, x_{s+t}) \mapsto (x_{\iota^{-1}(1)}, x_{\iota^{-1}(2)}, x_{\iota^{-1}(s)}, x_{\iota^{-1}(s+1)}, \dots, x_{\iota^{-1}(s+t)}).$$

Let the two disjoint submanifold  $X$  and  $Y$  of  $C_{s,t}$  satisfy  $\sigma(X) = Y$ . Then  $\int_X I(\Gamma) = \int_Y I(\Gamma)$  holds.

*Proof.*

$$\begin{aligned} & \int_Y I(\Gamma) \\ &= \int_{\sigma(X)} (\sigma^{-1})^* I(\Gamma), \end{aligned}$$

since the changes of signs are canceled.  $\square$

**Lemma 6.2** (Localizing lemma). Let  $\Gamma$  be a BCR graph with order  $k$ ,  $\#B(\Gamma) = s$  and  $\#W(\Gamma) = t$ . Let  $\psi$  be a generalized ribbon cycle with links  $p_1, \dots, p_k$ . Remember that each link consists of the image of a ball  $D_{p_i}$  (or  $D_{p_i}(\theta'_{\tau^{-1}(2i-1)})$ ) and the image of an annulus  $I \times S_{p_i}$ . Let  $C_0$  be the subspace of  $C_{s,t}(\psi)$  which consists of configurations  $(x_1, x_2, \dots, x_s, x_{s+1}, \dots, x_{s+t})$  satisfying the following.

- There exists  $i$  such that  $D_{p_i}$  or  $I \times S_{p_i}$  does not have any black vertex.

Then  $\int_{C_0} I(\Gamma) = 0$  holds.

*Proof.* Let  $p_i$  be such a link. Then the contribution of the integral vanishes by dimensional reason (or is canceled) with respect to the parameter  $y_i$  of (a family of) link  $p_i$ .  $\square$

Set

$$X_\alpha = \begin{cases} D_{p_i} \text{ or } D_{p_i}(\theta'_{\tau^{-1}(2i-1)}) & \text{if } \alpha = 2i - 1 \\ I \times S_{p_i} & \text{if } \alpha = 2i. \end{cases}$$

By Localizing lemma, we only consider the graph with  $s = 2k$  and  $t = 0$ , and configurations that there are some black vertex  $x_{\sigma^{-1}(\alpha)}$  in  $X_\alpha$ . We write the set of these configurations as  $C_\sigma$ ,  $\sigma \in \mathfrak{S}_{2\alpha}$ . If  $\sigma \neq \tau$ ,  $C_\sigma$  and  $C_\tau$  are not connected.

**Lemma 6.3** (Pairing lemma). If  $x_{\sigma^{-1}(2i-1)} \in D_{p_i}$  and  $x_{\sigma^{-1}(2i)} \in I \times S_{p_i}$  are not connected by dashed edges,  $\int_{C_\sigma} I(\Gamma) = 0$  holds.

*Proof.* This can be shown by a similar dimensional reason to the proof of Lemma 6.2.  $\square$

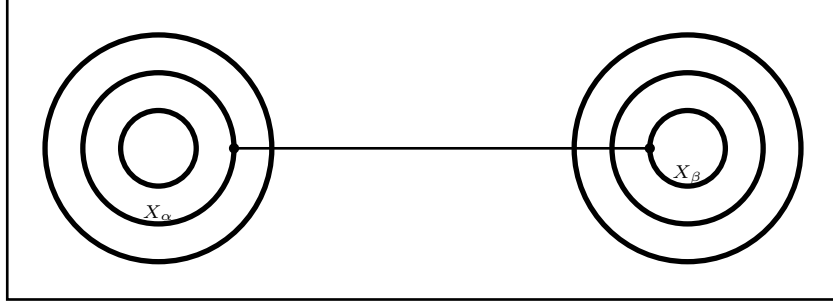


Figure 11: An edge connecting different systems

**Lemma 6.4** (Same system lemma). Let  $\Gamma$  be a BCR graph with order  $k$  (and defect 0),  $\#B(\Gamma) = 2k$  and  $\#W(\Gamma) = 0$ . Let  $\psi$  be a generalized ribbon cycle with crossings  $p_1, \dots, p_k$ . If  $X_\alpha$  and  $X_\beta$  are in different planetary systems, and  $x_{\sigma^{-1}(\alpha)}$  and  $x_{\sigma^{-1}(\beta)}$  are connected by solid edges (see Figure 11),  $\int_{C_\sigma} I(\Gamma) = 0$  holds.

*Proof.* This is because  $\frac{x_{\sigma^{-1}(\beta)} - x_{\sigma^{-1}(\alpha)}}{\|x_{\sigma^{-1}(\beta)} - x_{\sigma^{-1}(\alpha)}\|} \in S^{j-1}$  varies in a small neighborhood of a point in  $S^{j-1}$ .  $\square$

**Remark 6.5.** More precisely,  $\int_{C_\sigma} I(\Gamma) = 0$  above means  $\int_{C_\sigma} I(\Gamma)$  approach 0 as the radii of the two planetary systems approaches 0.

**Lemma 6.6** (Ingoing lemma). Let  $\Gamma$  be a BCR graph with order  $k$ ,  $\#B(\Gamma) = 2k$  and  $\#W(\Gamma) = 0$ . Let  $\psi$  be a generalized ribbon cycle with crossings(pairings)  $p_1, \dots, p_k$ . Let  $X_\alpha$  be a planetary orbit in a planetary system. Assume that all solid edges adjacent to  $x_{\sigma^{-1}(\alpha)}$  are outgoing. That is, if  $x_{\sigma^{-1}(\alpha)}$  and  $x_{\sigma^{-1}(\beta)}$  are connected by solid edges,  $X_\beta$  is outside  $X_\alpha$  (see Figure 12). Then  $\int_{C_\sigma} I(\Gamma) = 0$ .

*Proof.* Since the integrand form does not depend on the parameter  $x_{\sigma^{-1}(\alpha)}$ , it factors through  $C_\sigma \rightarrow C_\sigma / X_\alpha$ .  $\square$

**Lemma 6.7** (Decomposing lemma). • Let  $e = \{\sigma^{-1}(\alpha), \sigma^{-1}(\beta)\}$  be a solid edge. Let  $X_\alpha$  and  $X_\beta$  be in the same planetary system and  $X_\beta$  be outside. Then if  $X_\beta = I \times S_p$ ,  $\phi_e^* \omega_{S^{j-1}}$  depends only on the variable  $\theta_{\sigma^{-1}(\beta)} \in S_p$  of  $x_{\sigma^{-1}(\beta)} = (r_{\sigma^{-1}(\beta)}, \theta_{\sigma^{-1}(\beta)}) \in X_\beta$ . If  $X_\beta = D_p(\theta')$ , it depends only on  $\theta'$ .

• Let  $e = \{\sigma^{-1}(\alpha), \sigma^{-1}(\beta)\}$  be a dashed edge. Let  $X_\alpha = D_p$  (or  $D_p(\theta')$ ) and  $X_\beta = I \times S_p$ . Then  $\phi_e^* \omega_{S^{n-1}}$  depends on only on the variable  $x_{\sigma^{-1}(\alpha)} \in X_\alpha$  and on the first factor  $r_{\sigma^{-1}(\beta)} \in I$  of  $x_{\sigma^{-1}(\beta)} = (r_{\sigma^{-1}(\beta)}, \theta_{\sigma^{-1}(\beta)}) \in X_\beta$ .

*Proof.* This follows from the way we choose the scaling of planetary orbits.  $\square$

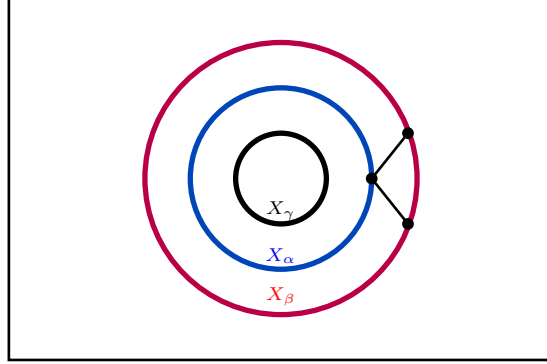


Figure 12: Outgoing edges

**Definition 6.8** (Graph-chord pairing). Let  $C$  be a chord diagram on directed lines with order  $k$ . Let  $\Gamma$  be a colored BCR graph with order  $k$ . Then the pairing  $\langle \Gamma, C \rangle$  is defined by counting as follows. First, we only count when

(I)  $\#B(\Gamma) = 2k (= \#V(C))$ .

Let  $\#B(\Gamma) = \#V(C) = 2k$ . We count permutations  $\sigma : \#B(\Gamma) \rightarrow \#V(C)$  which satisfies (I) and all the followings.

(II)  $\sigma$  induces the map  $\bar{\sigma} : E(\Gamma) \rightarrow E(C)$ .

(III) If two black vertices  $v_1$  and  $v_2$  are in the same solid component,  $\sigma(v_1)$  and  $\sigma(v_2)$  are in the same directed line.

(IV) If a vertex  $w$  of  $V(C)$  is off  $x$ -axis,  $w$  has an ingoing solid edge: there exists a vertex  $w'$  lower on the same directed line such that  $\sigma^{-1}(w)$  and  $\sigma^{-1}(w')$  are connected by some solid edge of  $\Gamma$ .

The sign of the counting is  $+1$  iff the orientation of  $\Gamma$  coincides with the induced orientation determined by the induced color from  $\sigma$  (See Definition 6.9).

**Definition 6.9** (Induced color on BCR diagrams). Let  $\sigma : B(\Gamma) \rightarrow V(C)$  satisfy all the conditions (I)(II)(III)(IV) of Definition 6.8. Then  $\sigma$  defines an induced color on the underlying graph  $\bar{\Gamma}$  in a natural way: we label black vertices using  $\sigma$  and the label of  $V(C)$ . We orient solid edges so that the orientations are compatible with directed lines. We orient dashed edges so that the orientations are compatible with those of chords. We label edges in the following order.

- (1) Ingoing solid edge (if it exists) from the initial vertex of the  $i$ th chord ( $i = 1, \dots, k$ ). There are  $g - 1$  solid edges ordered by this first step.
- (2) The  $\bar{\sigma}^{-1}(i)$ th dashed edge and the ingoing solid edge from the endpoint of the  $i$ th chord ( $i = 1, \dots, k$ )

**Theorem 6.10.** Let  $C$  be a chord diagram with order  $k$  associated with a generalized ribbon cycle  $\psi$ . Assume  $r(c)$  chords have negative sign. Let  $\Gamma$  be a BCR graph with order  $k$ . Then the value of the integral  $I(\Gamma)$  on  $\psi$  is equal to the pairing  $(-1)^{r(c)} < \Gamma, C >$ .

*Proof.* By (I) Localizing lemma 6.2 (II) pairing lemma 6.3, (III) Same system lemma 6.4, (IV) Ingoing lemma 6.6, the integral survives only on  $C_\sigma$  for  $\sigma$  which satisfies (I) (II) (III) (IV) of Definition 6.8. By Decomposing lemma 6.7 the integral on  $C_\sigma$  can be written as

$$\pm(-1)^{r(c)} \left( \int_{\theta'_j \in S} \bigwedge_{j=1}^{g-1} \eta_{\tau(j)} \right) \left( \bigwedge_i \int_{x_{\sigma^{-1}(2i)} \in D_{p_i}} \int_{r_{\sigma^{-1}(2i+1)} \in I} \omega_{p_i} \int_{\theta_{\sigma^{-1}(2i+1)} \in S_{p_i}} \eta_{p_i} \right).$$

Here  $\omega_{p_i}$  is the form associated with the edge  $\{x_{\sigma^{-1}(2i)}, x_{\sigma^{-1}(2i+1)}\}$ .  $\eta_{p_i}$  is the form associated with the edge that goes down from  $x_{\sigma^{-1}(2i+1)}$ .  $\eta_{\tau(j)}$  is the form associated with the edge that goes down from  $x_{\tau(j)}$ . The sign at the head is  $+$  if the orientation of configuration space  $C_\sigma$  coincides with the orientation induced by the coordinate  $(x_{\sigma^{-1}(1)}, x_{\sigma^{-1}(2)}, \dots, x_{\sigma^{-1}(2k)})$ , and also  $\omega$  is exactly  $\bigwedge_{j=1}^{g-1} \eta_{p_{\tau(j)}} \bigwedge (\omega_{p_i} \eta_{p_i})$

In the part  $\int_{r \in I} \int_{x \in D} \theta$ , the linking number of  $D$  and  $I$  is computed, which is 1 or  $-1$  depending on sign of the chord.  $\square$

**Notation 6.11.** Let  $C$  be a chord diagram on directed lines. Let  $G(C)$  be the set of BCR graphs (without color) mapped on  $C$  satisfying all the conditions of Definition 6.8.

**Lemma 6.12.**  $G(C)$  consists of  $\sum_{i=1}^s 2^{t_i-1}$  graphs.

*Proof.* Since dashed edges must be mapped on chords, the remaining choices are solid edges. The top vertex  $v$  on each directed line must be one of the ends of some solid component. The solid component first goes down from  $v$  to  $O$  through some of the vertices on the directed line. After reaching  $O$ , the solid component goes up through the remaining vertices. We can choose which  $t_i - 1$  vertices between  $v$  and  $O$  the solid component passes when it goes down.  $\square$

**Theorem 6.13** (Counting formula). Let  $H$  be a graph cocycle that consists of  $g$ -loop graphs with order  $k$ . Let  $C$  be a chord diagram on directed lines with order  $k$  with  $r(C)$  chords negative sign. Let  $\psi$  be a generalized ribbon cycle constructed from  $C$ . Then

$$I(H)(\psi) = (-1)^{r(C)} \sum_{\bar{\Gamma} \in G(C)} w(\Gamma) \text{Aut}(\bar{\Gamma}) s(\Gamma, \bar{\Gamma}).$$

Here  $\Gamma$  is a choice of a colored graph in  $H$  such that the underling graph of  $\Gamma$  is  $\bar{\Gamma}$ . The sign  $s(\Gamma, \bar{\Gamma}) \in \{+1, -1\}$  is 1 iff the orientation of  $\Gamma$  coincides with that of  $\bar{\Gamma}$  with induced color.

*Proof.* This follows from Theorem 6.10 and Symmetry lemma 6.1.  $\square$

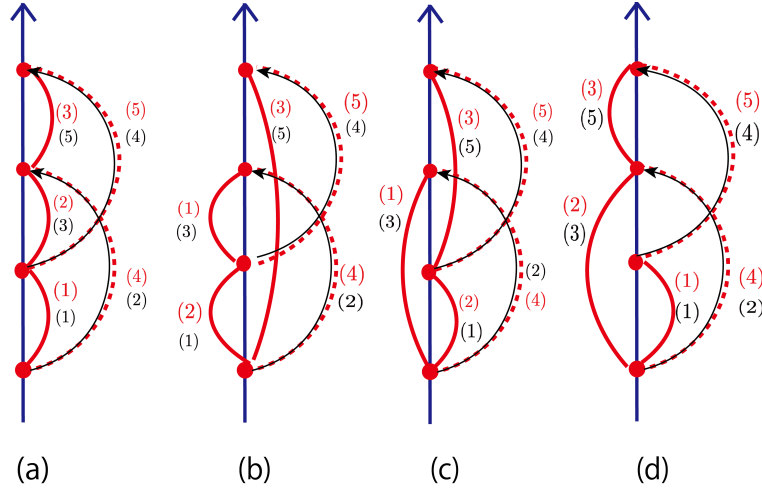
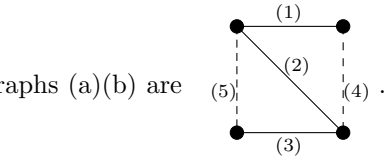
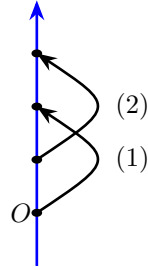


Figure 13: BCR graphs of  $G(C_1)$

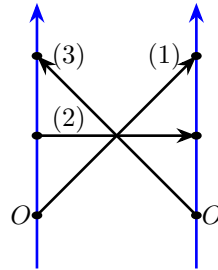
**Example 6.14.** For the chord diagram  $C_1 =$



the four graphs in Figure 13. The first two graphs (a)(b) are

The last two graphs do not appear in the graph cocycle  $H_1$ , because they are not admissible graphs. The induced color is written in black. The sign  $s(\Gamma, \bar{\Gamma})$  is (a)  $-1$ (b)  $+1$ .

**Example 6.15.** For the chord diagram  $C_2 =$



,  $G(C_2)$  con-

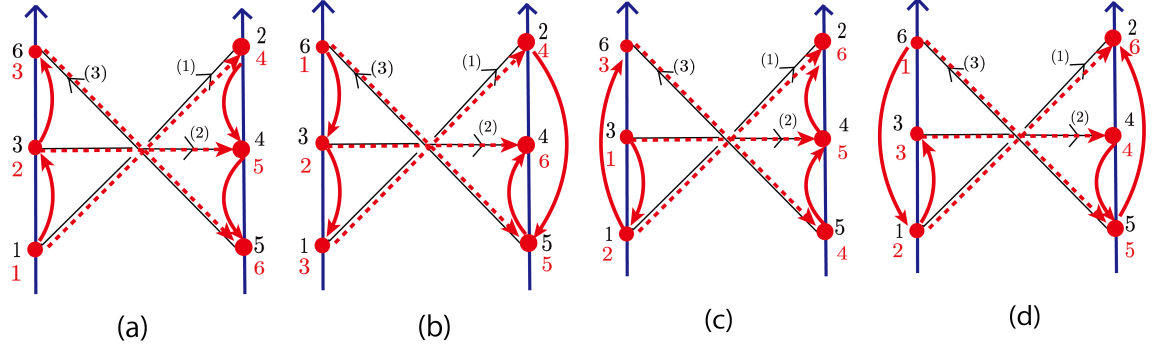
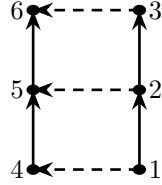
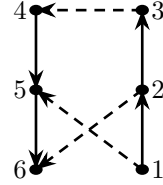


Figure 14: BCR graphs of  $G(C_2)$

sists of the four graphs drawn in red in Figure 14. The first BCR graph (a) is



The other three graphs (b) (c) (d) are



induced color is written in black. The sign  $s(\Gamma, \bar{\Gamma})$  is (a)  $-1$  (b)  $+1$  (c)  $+1$  (d)  $-1$  respectively.

Finally, we see a lemma for canceling the contribution of the collection terms.

**Definition 6.16.** We write  $\bar{\psi}(p_1, p_2, \dots, p_n)$  for the cycle obtained from  $\bar{\psi}$  by resolving ribbon links  $p_1, p_2, \dots, p_n$  (Figure 15). Set

$$\bar{\psi}[p_1, p_2, \dots, p_k] = \sum_{I \subset \{1, \dots, k\}} (-1)^{\#I} \bar{\psi}(\{p_i, i \in I\}).$$

**Lemma 6.17.**  $\bar{c}(H)(\bar{\psi}[p_1, p_2, \dots, p_k]) = 0$

*Proof.* Remember that  $c(H)$  (or  $\bar{c}(H)$ ) only depends on  $D : C_1(\mathbb{R}^j) \rightarrow \text{Inj}(\mathbb{R}^j, \mathbb{R}^n)$  (or  $\bar{D} : [0, 1] \times C_1(\mathbb{R}^j) \times \text{Emb}(\mathbb{R}^j, \mathbb{R}^n) \rightarrow \text{Inj}(\mathbb{R}^j, \mathbb{R}^n)$ ). Hence the contribution of  $\bar{c}(H)$  cancels before and after the resolution of each link.  $\square$

## 7 Proof of Main Result

Finally, we perform pairing between the cocycles given in Section 4 and the cycles given in Section 5, and prove Main Result.

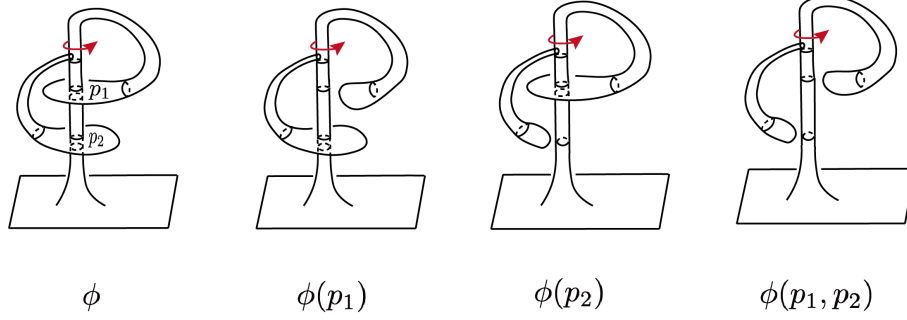


Figure 15: Resolving ribbon links

**Theorem 7.1.**

$$\bar{z}_2^2(\bar{\phi}[p_1, p_2]) = \bar{z}_2^2(\bar{\phi} + \bar{\phi}(p_1) - \bar{\phi}(p_2) - \bar{\phi}(p_1, p_2)) = 0.$$

**Remark 7.2.** The above theorem certainly makes sense since the  $(j-1)$ -parameter family  $\phi$  of long knots has the trivial image in  $\pi_{2n-j-5}\text{Emb}(S^j, S^n)_u$ .

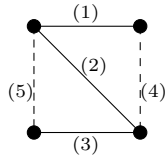
**Theorem 7.3.**

$$\bar{z}_2^3(\bar{\psi}[p_1, p_2, p_3]) = 1.$$

*proof of Theorem 7.1.*

$$\begin{aligned} \bar{z}_2^2(\bar{\phi}[p, q]) &= \bar{z}_2^2(\bar{\phi} + \bar{\phi}(p_1) - \bar{\phi}(p_2) - \bar{\phi}(p_1, p_2)) \\ &= (r^*I(H) + \bar{c}(H))(\bar{\phi} + \bar{\phi}(p_1) - \bar{\phi}(p_2) - \bar{\phi}(p_1, p_2)) \\ &= I(H)(\phi + \phi(p_1) - \phi(p_2) - \phi(p_1, p_2)) \end{aligned}$$

by lemma 6.17. By dimensional reason  $I(H)(\phi + \phi(p_1) - \phi(p_2) - \phi(p_1, p_2))$  is equal to  $I(H)(\phi)$ . To compute  $I(H)(\phi)$ , we use Counting formula 6.13. Note

that the underlining graph of  has 2 automorphisms. In the

graph cocycle  $H_1$ ,  $w(\begin{smallmatrix} (1) \\ (5) \end{smallmatrix} \begin{smallmatrix} (2) \\ (4) \end{smallmatrix} \begin{smallmatrix} (3) \end{smallmatrix}) = \frac{1}{2}$ . Hence

$$I(H_1)(\psi) = - \sum_{\bar{\Gamma} \in G(C)} w(\Gamma) \text{Aut}(\bar{\Gamma}) s(\Gamma, \bar{\Gamma}) = -\frac{1}{2} \times 2 \times (-1 + 1) = 0.$$

□

*proof of Theorem 7.3.* By similar argument to proof of Theorem 7.1,  $\bar{z}_2^3(\bar{\psi}[p_1, p_2, p_3]) =$

$I(H)(\psi)$ . Note that the underlining graph of  $\begin{smallmatrix} 6 & \leftarrow & 3 \\ 5 & \leftarrow & 2 \\ 4 & \leftarrow & 1 \end{smallmatrix}$  has 4 automor-

phisms, and the underlining graph of  $\begin{smallmatrix} 4 & \leftarrow & 3 \\ 5 & \leftarrow & 2 \\ 6 & \leftarrow & 1 \end{smallmatrix}$  has 2 automorphisms. In

the graph cocycle  $H_2$ ,  $w(\begin{smallmatrix} 6 & \leftarrow & 3 \\ 5 & \leftarrow & 2 \\ 4 & \leftarrow & 1 \end{smallmatrix}) = -\frac{1}{4}$  and  $w(\begin{smallmatrix} 4 & \leftarrow & 3 \\ 5 & \leftarrow & 2 \\ 6 & \leftarrow & 1 \end{smallmatrix}) = -1$ .

Hence by Counting formula 6.13,

$$I(H_2)(\psi) = - \sum_{\bar{\Gamma} \in G(C)} w(\Gamma) \text{Aut}(\bar{\Gamma}) s(\Gamma, \bar{\Gamma}) = -(-\frac{1}{4} \times 4 \times (-1) + (-1) \times 2 \times (+1 + 1 - 1)) = 1.$$

□

**Remark 7.4.** From the above argument, we can check Arnol'd relation holds.

$$I \left( \begin{smallmatrix} 6 & \leftarrow & 3 \\ 5 & \leftarrow & 2 \\ 4 & \leftarrow & 1 \end{smallmatrix} \right) + 2I \left( \begin{smallmatrix} 4 & \leftarrow & 3 \\ 5 & \leftarrow & 2 \\ 6 & \leftarrow & 1 \end{smallmatrix} \right) = (-4) + 2 \times 2 = 0.$$



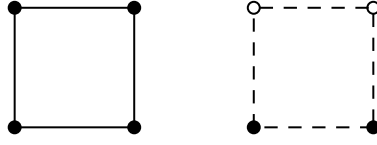
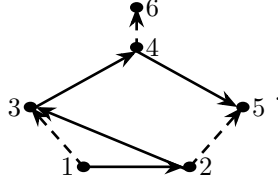


Figure 16: Example of solid and dashed loops

**Remark 7.5.** It is likely we can take a non-trivial cycle from other components

using other graphs of  $H_2$ , for example,



## 8 Higher orders and higher loops

There are further problems to be tackled regarding more general graphs. Let  $g$  be the number of loops of a graph and  $k$  be the order of it.

- Use graphs with  $g \geq 3$  to show the non-triviality of  $\pi_{g-1}(\text{Emb}_{\partial}(D^2, D^4)_u)$ , which are of higher degree than that of [BG] and [Wat 6].
- Use Graphs with  $k \geq 3$  to construct a non-trivial infinite-rank subgroup of  $\pi_1(\text{Emb}_{\partial}(D^2, D^4)_u)$  through 2-loop graphs, following [BG] and [Wat 6].

So far, when  $(n, j) = (\text{even}, \text{even})$ , we have already computed the top ( $l = 0$ ) of the graph cohomology for  $(k, g) = (3, 2), (3, 3), (4, 4)$ . However, all of them turn out to be trivial. For  $(k, g) = (4, 2), (5, 5)$  we can expect we obtain non-trivial graph cocycles. To give necessary conditions of non-triviality of the graph cohomology, we introduce a modified BCR graph complex. We emphasize that the modified BCR complex plays an essential role only when  $g \geq 2$ .

### 8.1 The modified BCR graph complex

**Definition 8.1.** A solid (and dashed) loop is a loop which consists of only solid (and dashed, respectively) edges. Dashed edges are allowed to contain black vertices. Small or double loops are not counted as loops. A BCR graph  $\Gamma$  is said to be good if it has neither solid loops nor dashed loops. See Figure 16.

**Definition 8.2.** Let  $\overline{\mathcal{D}}_g^{k,l}$  be the complex of good BCR graphs. That is, we impose the further relation  $\Gamma = 0$  for each non-good graph  $\Gamma$ . Let  $\mathcal{D}'_g^{k,l}$  be the subcomplex of  $\mathcal{D}_g^{k,l}$  which consists of all non-good graphs.

$$\begin{array}{ccccccc}
& 0 & & 0 & & 0 & \\
& \downarrow & & \downarrow & & \downarrow & \\
0 & \longleftarrow \overline{\mathcal{D}}_g^{k,0} & \xleftarrow{\pi} & \mathcal{D}_g^{k,0} & \xleftarrow{i} & \mathcal{D}'_g^{k,0} & \longleftarrow 0 \\
& \downarrow & & \downarrow & & \downarrow & \\
0 & \longleftarrow \overline{\mathcal{D}}_g^{k,1} & \xleftarrow{\pi} & \mathcal{D}_g^{k,1} & \xleftarrow{i} & \mathcal{D}'_g^{k,1} & \longleftarrow 0 \\
& \downarrow & & \downarrow & & \downarrow & \\
0 & \longleftarrow \overline{\mathcal{D}}_g^{k,2} & \xleftarrow{\pi} & \mathcal{D}_g^{k,2} & \xleftarrow{i} & \mathcal{D}'_g^{k,2} & \longleftarrow 0 \\
& \downarrow & & \downarrow & & \downarrow &
\end{array}$$

Figure 17: Exact sequence of  $\overline{\mathcal{D}}_g^{k,*}$ ,  $\mathcal{D}_g^{k,*}$  and  $\mathcal{D}'_g^{k,*}$

**Lemma 8.3.** We get the diagram of Figure 17, where the horizontal sequences are exact and the vertical sequences are cochain complexes.

Hence we have a long cohomology exact sequence

$$0 \rightarrow H^0(\mathcal{D}'_g^{k,*}) \rightarrow H^0(\mathcal{D}_g^{k,*}) \rightarrow H^0(\overline{\mathcal{D}}_g^{k,*}) \rightarrow H^1(\mathcal{D}'_g^{k,*}) \rightarrow \dots$$

If  $j$  (and  $n$ ) is large enough, by using a non-trivial graph cocycle of  $\overline{\mathcal{D}}_g^{k,0}$  instead of  $\mathcal{D}_g^{k,0}$ , we would be able to obtain non-trivial cocycles of  $\text{Emb}_\partial(D^j, D^n)$ . The reason why we can exclude non-good graphs in this stable range is the following.

**Lemma 8.4.** Let  $\Gamma$  be a non-good graph. Let

$$\phi(\Gamma) : C_{s,t} \rightarrow (S^j)^{\#E_\eta(\Gamma)} \times (S^n)^{\#E_\theta(\Gamma)}$$

be the direction map (Definition 2.24) from configuration space bundle over  $\text{Emb}(\mathbb{R}^j, \mathbb{R}^n)$ . Then there exists  $J$  such that for  $j \geq J$ , the image of  $\phi(\Gamma)$  has codimension larger than 1. Hence  $\omega(\Gamma) = \phi(\Gamma)^* \wedge \omega_{S^j} \wedge \omega_{S^n}$  factors through codimension  $\geq 2$  subspace  $A \subset (S^j)^{\#E_\eta(\Gamma)} \times (S^n)^{\#E_\theta(\Gamma)}$ .

**Question 8.5.** Does  $H^0(\mathcal{D}_g^{k,*}) \cong H^0(\overline{\mathcal{D}}_g^{k,*})$  hold ?

**Remark 8.6.** The modified graph complex  $\overline{\mathcal{D}}_g^{k,*}$  seems to be closer to the graph complex  $HH$  of Arone-Turchin [AT1][AT2], which arises from homotopy

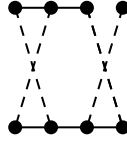


Figure 18: Graph  $G$

theoretical approach, in the sense their complex does not admit solid or dashed loops. Relation between the two approaches which give similar graph complexes are to my knowledge still unknown, though there are some progress by Volić [Vol] in the case of 1-dimensional knots.

**Remark 8.7.** So far the author has no idea to give a lower bound of  $H^0(\mathcal{D}_g^{k,*})$  or  $H^0(\overline{\mathcal{D}}_g^{k,*})$  using some algebraic structure as the Jacobi diagram case [Bar].

The modified BCR graph cohomology is much easier to calculate. This is because we do not have to contract dashed edges that connect two “solid-connected” black vertices as well as solid edges that connect two “dotted-connected” black vertices. This argument is particularly helpful when  $k - g$  is small.

## 8.2 Computation of some modified BCR graph cohomology

By computer calculus using Python, we have obtained the following result.

**Proposition 8.8.**  $H^0(\overline{\mathcal{D}}_2^{4,*})$  is 1-dimensional.  $H^0(\overline{\mathcal{D}}_5^{5,*})$  is 3-dimensional.

**Proposition 8.9.** The basis of  $H^0(\overline{\mathcal{D}}_2^{4,*})$  is given by  $H_3 = G + (\text{a linear combination of other 54 graphs})$ . The basis of  $H^0(\overline{\mathcal{D}}_5^{5,*})$  is given by

$$\begin{aligned} H_4 &= 1\Gamma_1 + 0\Gamma_2 + 0\Gamma_3 + (\text{a linear combination of other 693 graphs}). \\ H_5 &= 0\Gamma_1 + 1\Gamma_2 + 0\Gamma_3 + (\text{a linear combination of other 446 graphs}). \\ H_6 &= 0\Gamma_1 + 0\Gamma_2 + 1\Gamma_3 + (\text{a linear combination of other 138 graphs}). \end{aligned}$$

See Figure 18 and 19 for the definition of  $G, \Gamma_1, \Gamma_2, \Gamma_3$  (suitable edge labels should be chosen). See Figure 21 for the full list of graphs (and their coefficients) in  $H_3$ , where  $G = G_{14}$ .

**Remark 8.10.** There is one hidden face of  $H_3$  that can not be canceled or vanish by the argument of subsection 4.2. This is the face (of  $G_{50}$ ) in Figure 20. However, we can handle this specific face individually, because the quotient graph  $\Gamma/\Gamma_A$  has a symmetry. On the other hand, we may need more effort to cancel the hidden faces of  $H_4$ ,  $H_5$  and  $H_6$ .



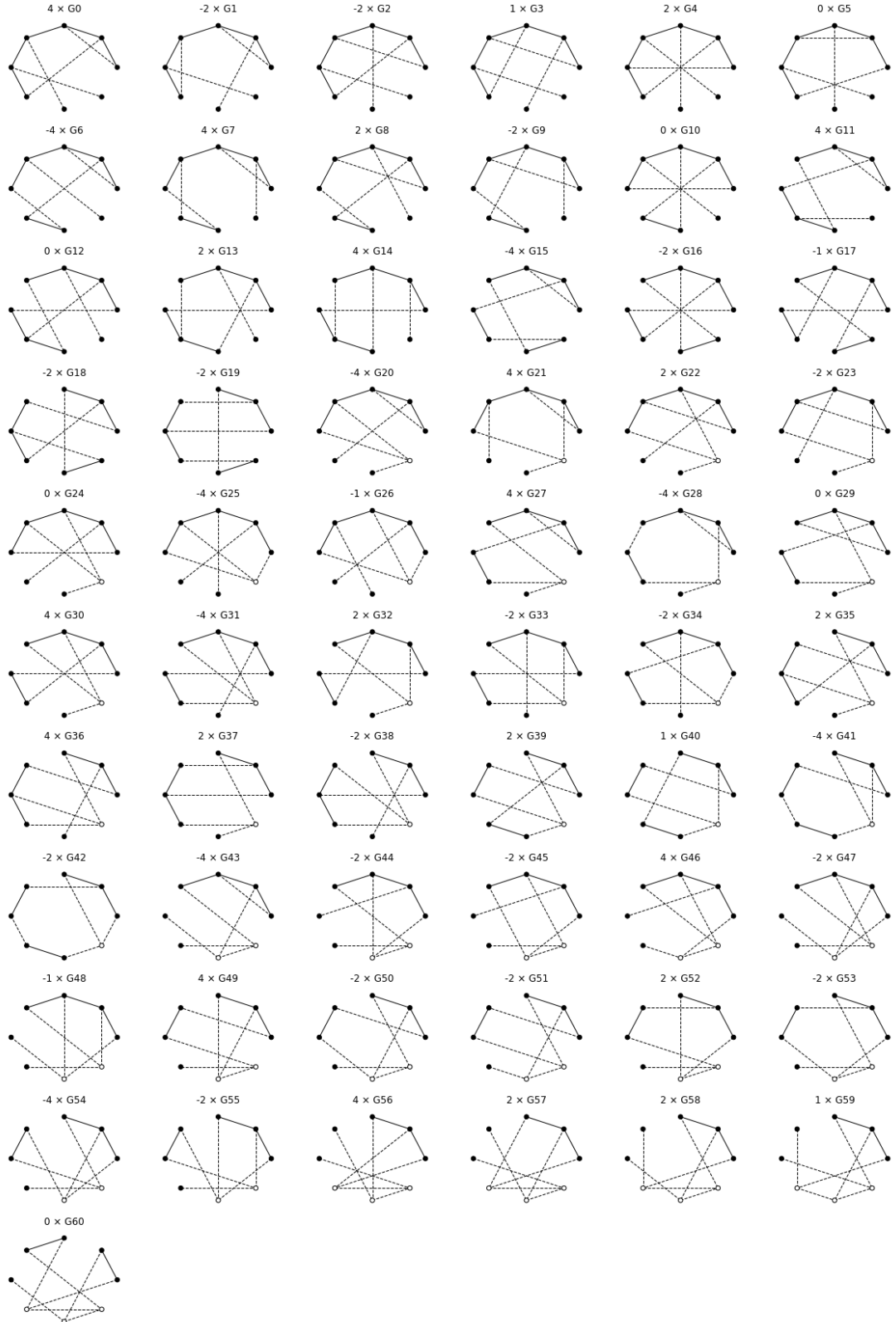


Figure 21: Non-trivial graph cocycle  $H_3$

## References

- [Arn] V. Arnol'd, *The cohomology ring of the colored braid group*. Mathematical Notes of the Academy of Sciences of the USSR 5, 138–140 (1969).
- [AS] S. Axelrod, I. M. Singer, *Chern-Simons perturbation theory. II*. J. Differential Geom. 39 (1994), no. 1, 173–213.
- [AT1] G. Arone, V. Turchin, *On the rational homology of high-dimensional analogues of spaces of long knots*. Geom. Topol. 18 (2014), no. 3, 1261–1322.
- [AT2] G. Arone, V. Turchin, *Graph-complexes computing the rational homotopy of high dimensional analogues of spaces of long knots*. Ann. Inst. Fourier (Grenoble) 65 (2015), no. 1, 1–62.
- [Bar] D. Bar-Natan, *On the Vassiliev knot invariants*. Topology 34 (1995), no. 2, 423–472.
- [BG] R. Budney, D. Gabai, *Knotted 3-balls in  $S^4$* . arXiv.1912.09029
- [Bud] R. Budney, *A family of embedding spaces*. Geometry and Topology Monographs 13 (2008) 41–83.
- [Bot] R. Bott, *Configuration spaces and imbedding invariants*. Turkish J. Math. 20 (1996), no. 1, 1–17.
- [BT] R. Bott, C. Taubes, *On the self-linking of knots*. Topology and physics. J. Math. Phys. 35 (1994), no. 10, 5247–5287.
- [CCTW] J. Conant, J. Costello, V. Turchin, P. Weed, *Two-loop part of the rational homotopy of spaces of long embeddings*, J. Knot Theory Ramifications 23,(2014), no. 4, 1450018, 23 pp.
- [Cer] J. Cerf, *Topologie de certains espaces de plongements*. Bull. Soc. Math. France 89 (1961), 227–380.
- [CCL] A. Cattaneo, P. Cotta-Ramusino, R. Longoni, *Configuration spaces and Vassiliev classes in any dimension*. Algebr. Geom. Topol. 2 (2002), 949–1000.
- [CR] A. S. Cattaneo, C. A. Rossi, *Wilson surfaces and higher dimensional knot invariants*. Comm. Math. Phys. 256 (2005), no. 3, 513–537
- [FTW] B. Fresse, V. Turchin, T. Willwacher, *The rational homotopy of mapping space of  $E_n$  operads*, arXiv.1703.06123
- [GGP] S. Garoufalidis, M. Goussarov, M. Polyak, *Calculus of clovers and finite type invariants of 3-manifolds*. Geom. Topol. 5 (2001), 75–108.
- [GW] T. Goodwillie, M. Weiss, *Embeddings from the point of view of immersion theory. II*. Geom. Topol. 3 (1999), 103–118.

- [GKW] T. Goodwillie, J. Klein, M. Weiss. *Spaces of smooth embeddings, disjunction and surgery*. Surveys on surgery theory, Vol. 2, 221–284, Ann. of Math. Stud., 149, Princeton Univ. Press, Princeton, NJ, 2001.
- [Hab] K. Habiro, *Claspers and finite type invariants of links*. Geom. Topol. 4 (2000), 1–83.
- [HKS] K. Habiro, T. Kanenobu, A. Shima, *Finite type invariants of ribbon 2-knots*. Low-dimensional topology (Funchal, 1998), 187–196, Contemp. Math., 233, Amer. Math. Soc., Providence, RI, 1999.
- [Kon] M. Kontsevich, *Feynman diagrams and low-dimensional topology*. First European Congress of Mathematics, Vol. II (Paris, 1992), 97–121, Progr. Math., 120, Birkhäuser, Basel, 1994.
- [KT] G. Kuperberg, D. Thurston, *Perturbative 3-manifold invariants and cut-and-paste topology*. math.GT.9912167
- [Les 1] C. Lescop, *On the Kontsevich-Kuperberg-Thurston construction of a configuration-space invariant for rational homology 3-spheres*. math.GT.0411088
- [Les 2] C. Lescop, *Splitting formulae for the Kontsevich-Kuperberg-Thurston invariant for rational homology 3-spheres*. math.GT.0411431
- [Les 3] C. Lescop, *Invariants of links and 3-manifolds from graph configurations*. arXiv.2001.09929
- [Let] D. Leturcq, *Generalized Bott-Cattaneo-Rossi invariants of high dimensional long knots*. J.Math. Soc. Japan 73 (2021), no.3, 815–860.
- [MT] M. Mimura, H. Toda *Topology of Lie groups. I, II*. Translations of Mathematical Monographs, 91. American Mathematical Society, Providence, RI, 1991.
- [Pal] R. Palais, *Local triviality of the restriction map for embeddings*. Comment. Math. Helv. 34 (1960), 305–312.
- [Sak 1] K. Sakai, *Nontrivalent graph cocycle and cohomology of the long knot space*. Algebr. Geom. Topol. 8 (2008), no. 3, 1499–1522.
- [Sak 2] K. Sakai, *Configuration space integrals for embedding spaces and the Haefliger invariant*. J. Knot Theory Ramifications 19 (2010), no. 12, 1597–1644.
- [Sak 3] K. Sakai, *An integral expression of the first nontrivial one-cocycle of the space of long knots in  $\mathbb{R}^3$* . Pacific J. Math. 250 (2011), no. 2, 407–419.
- [SW] K. Sakai, T. Watanabe, *1-loop graphs and configuration space integral for embedding spaces*. Math. Proc. Cambridge Philos. Soc. 152 (2012), no. 3, 497–533.

- [Sin] D.P. Sinha, *The topology of spaces of knots: cosimplicial models*. Amer. J. Math. 131 (2009), no. 4, 945–980.
- [Sin2] D.P. Sinha, *The homology of the little discs operad*. Séminaire et Congrès de Société Mathématique de France 26 (2011), p. 255–281.
- [Vol] I. Volić, *Configuration space integrals and Taylor towers for spaces of knots*. Topology Appl. 153 (2006), no. 15, 2893–2904.
- [Wat 1] T. Watanabe, *Configuration space integral for long  $n$ -knots and the Alexander polynomial*. Algebr. Geom. Topol. 7 (2007), 47–92.
- [Wat 2] T. Watanabe, *On Kontsevich’s characteristic classes for higher dimensional sphere bundles. I. The simplest class*. Math. Z. 262 (2009), no. 3, 683–712.
- [Wat 3] T. Watanabe, *On Kontsevich’s characteristic classes for higher-dimensional sphere bundles. II. Higher classes*. J. Topol. 2 (2009), no. 3, 624–660.
- [Wat 4] T. Watanabe, T. Watanabe. *Higher order generalization of Fukaya’s Morse homotopy invariant of 3-manifolds I*. Invariants of homology 3-spheres. Asian J. Math. 22 (2018), no. 1, 111–180.
- [Wat 5] T. Watanabe, *Some exotic nontrivial elements of rational homotopy groups of  $\text{Diff}(S^4)$* . arxiv.1812.02448
- [Wat 6] T. Watanabe, *Theta-graph and diffeomorphisms of some 4-manifolds*. arXiv.2005.09545
- [Wei] M. Weiss, *Embeddings from the point of view of immersion theory I*. Geom. Topol. 3 (1999), 67–101.
- [Wit] E. Witten, *Quantum field theory and the Jones polynomial*, Comm. Math. Phys. 121(1989), no.3, 351–399.